Electronic Supplementary Material (ESI) for Nanoscale.
This journal is © The Royal Society of Chemistry 2020

Supporting Information

A Site-Specific Self-Assembled Light-up Rotor Probe for Selective Recognition and Stabilization of *c-MYC* G-Quadruplex DNA

Marco Deiana,[a] Karam Chand,[b] Jan Jamroskovic,[a] Rabindra Nath Das,[b] Ikenna Obi,[a] Erik Chorell,[*b] and Nasim Sabouri,[*a]

[a]Department of Medical Biochemistry and Biophysics, Umeå University, 90187 Umeå, Sweden

[b]Department of Chemistry, Umeå University, 90187 Umeå, Sweden

*Corresponding authors: erik.chorell@umu.se and nasim.sabouri@umu.se

Table of contents:

Experimental Procedures

General

Solvents, reagents, chemicals and biological templates were purchased from commercial suppliers (Sigma-Aldrich and Eurofins Genomics) and used without further modifications, unless otherwise stated. Oligonucleotides were diluted with ultrapure water to a concentration of 1 mM and stored at 5 °C. The exact oligonucleotide concentration was determined by UV/Vis spectroscopy using the molar extinction coefficients (ε_{260}) provided in Table S1 and calculated by using oligo analyzer on the IDT web site. For all the experiments involving biological samples, DNAse free water was used. A 1 M KCl stock solution was prepared by using solid KCl. The aqueous stock solution (0.5 M) of TRIS buffer was prepared by dissolving tris(hydroxymethyl)aminomethane in water and the pH was then adjusted to 7.5. The stock solutions of the synthesized compounds were prepared in DMSO at a final concentration of 10 mM. The final concentration of DMSO in all the DNA-based assays reached the maximum value of 2 % (v/v).

Absorption and steady-state emission spectra

Concentration- and temperature-dependent UV/Vis absorption spectra were recorded on T90+ UV/Vis spectrometer (PG instruments Ltd). Fluorescence spectra were recorded on Jasco FP-6500 spectrofluorometer equipped with the JascoPeltier-type temperature controller (ETC2736). The slits width of both monochromators were 5 nm. Relative fluorescence quantum yields (Φ_F) were determined by dilution method (OD_{max} < 0.1) using 5-(Dimethylamino)-1-naphthalenesulfonamide as reference standard (Φ_F = 5%, in water). Φ_F were calculated according to the following equation (Eq. S1):

$$\Phi_F = \Phi_F^{ref} \times \frac{I_\lambda}{I_\lambda^{ref}} \times \frac{OD_\lambda^{ref}}{OD_\lambda} \times \frac{\eta^2}{\eta_{ref}^2} \qquad (Eq.S1)$$

where I is the intensity emission area, OD is the optical density at the excitation wavelength and η is the refractive index of the solution. All optical measurements were performed in quartz cell cuvettes with conventional path lengths of 10 mm.

Electronic circular dichroism spectra

Electronic circular dichroism spectra were measured with a Jasco J-720 spectropolarimeter equipped with the JascoPeltier-type temperature controller (PTC-423L) and are presented as a sum of 4 accumulations. ECD spectra were performed in the range of 200-600 nm. Before use, the optical chamber of the CD spectrometer was deoxygenated with dry nitrogen and was held under nitrogen atmosphere during the measurements. Appropriate references were subtracted from the obtained ECD spectra. CD melting data were acquired by raising the temperature from 20 to 95 °C and monitoring the CD peak at 264 and 293 nm for *c-MYC* Pu22 and Tel-22, respectively. Prefolded oligonucleotides were diluted to a final concentration of 2.0 µM into 10 mM Tris pH 7.5 and 1 mM KCl. To confirm the G4 folding under these experimental conditions (i.e. 10 mM Tris pH 7.5 and 1 mM KCl) we recorded and compared the CD spectra of both *c-MYC* Pu22 and Tel-22 with those acquired by using 10 mM Tris pH 7.5 and 100 mM KCl (Figure S9 A and I). Melting values were estimated by fitting the normalized melting curves with a dose response function using OriginPro 2015 software.

Singlet lifetime measurements

Fluorescence lifetime decays were collected via Time-Correlated Single Photon Counting (TCSPC) setup by using a Fluorolog TCSPC (Horiba Jobin Yvon). The excitation source was a NanoLED-03 with a relatively broad excitation maximum centered at 375 nm. Lifetimes were obtained by monitoring the decay in the emission maximum (558 nm, emission slit 5.0 nm) upon insertion into the excitation path of an interference filter (365 nm, Melles Griot, The Netherlands). Time-resolved data were fitted with a triexponential function (Eq. S2):

$$I = A + B_1 e^{-\frac{t}{t_1}} + B_2 e^{-\frac{t}{t_2}} + B_3 e^{-\frac{t}{t_3}} \qquad (Eq.S2)$$

Then, the averaged fluorescence lifetimes were calculated according to Eq. S3:

$$< \tau > = \frac{\sum A_i \tau_i^2}{\sum A_i \tau_i} \qquad (Eq.S3)$$

where A_i is the *i-th* relative amplitude and τ_i is the *i-th* component of fluorescence lifetime, respectively.

Spectrophotometric titrations

A solution of **4b** 15.0 µM has been prepared by diluting the stock solution in the suitable amount of buffered water (% DMSO = 0.15 %, C_{KCl} = 100 mM, TRIS buffer 10.0 mM, pH = 7.5). The freshly prepared **4b** solution has been then titrated with the annealed oligonucleotide buffered solution and let to equilibrate for several minutes before recording the UV/Vis spectra.

Fluorimetric titrations

A solution of **4b** 2.5 µM has been prepared by diluting the stock solution in the suitable amount of buffered water (% DMSO = 0.025 %, C_{KCl} = 100 mM, TRIS buffer 10.0 mM, pH = 7.5). The freshly prepared **4b** solution has been then titrated with the annealed oligonucleotide buffered solution and let to equilibrate for several minutes before recording the emission spectra. The concentration of the experiments were optimized to have OD < 0.1 to avoid reabsorption in the fluorescence emission. All the emission spectra have been baseline corrected.

Data processing

All the data were corrected for the dilution upon titration. Binding constants were obtained with Bindfit (available on the website http://supramolecular.org/) by using multiple global fitting methods (Nelder-Mead method) of both the UV/Vis and fluorescence data in the range 320 – 360 and 485 – 615 nm, respectively. Dilution corrections option was included in the fitting option. In order to ensure to find the minima in the fitting analyses, all the fittings were confirmed with three different start values.[S1-S3]

G-tetrad selectivity

An equilibrium-binding assay mediated by **4b**-induced fluorescence quenching of Texas red (Txred, λ_{exc} = 596 nm) labelled to either the 5′- or 3′-ends of *c-MYC* Pu22 enabled qualitative interrogation of mutually exclusive binding interactions at opposed G-tetrads. [5′-Txred *c-MYC* Pu22] = [3′-Txred *c-MYC* Pu22] = 0.25 µM. G-tetrad selectivity in % is expressed as: $[(F/F_0) \cdot 100] - 100$, where F_0 and F are the emission intensities before and after **4b** addition.[S4]

LOD calculation

Limit of detection (LOD) experiment was performed exciting compound **4b** at 355 nm (isosbetic point) in order to avoid changes in the absorbance values. Sensitivity was calculated by plotting the changes in the emission maximum (558 nm) as a function of *c-MYC*-Pu22 concentration. LOD was calculated according to the following equation:[S5]

$$LOD = \frac{s_b \times k}{m} \qquad (Eq.S4)$$

where s_b is the standard deviation calculated out of 15 independent measurements on blank solution, k is 3, according to IUPAC recommendations and m is the slope obtianed from the linear fitting (I_{558} *vs.* [*c-MYC* Pu22]).

Aggregation studies

4b in pure water forms stable molecular aggregates even at low micromolar concentration. Therefore, concentration-dependent UV/Vis experiments were performed by increasing the concentration of **4b** in a water:MeOH (90:10) binary mixture. Changes on the apparent extinction coefficient at 317 nm were plotted as function of **4b** concentration. Data points were fitted by using an isodesmic binding model that provided an aggregation constant (K_{agg}) = 7.3 x 10^5 M^{-1}.

Variable-temperature spectrophotometric and fluorimetric experiments were performed by raising the temperature from 25 to 95 °C, with a 5 °C interval.

Solvent-dependent studies were performed by dissolving **4b** (15 and 2 μM for absorption and emission studies, respectively) in different organic solvents. Then, the changes of the emission maxima and extinction coefficient depending on the solvent polarity were plotted. In addition, different DMSO volume fraction $\chi_{(DMSO)}$ in water/DMSO mixtures were used to monitor the disaggregation behavior of **4b**.

Sodium dodecyl sulfate (SDS) experiments were carried out by adding to a **4b** water solution (15 and 2.5 μM for absorption and emission studies, respectively) SDS 0.5 M.

Ionic strength dependence was assessed by titrating **4b** (15 μM) with increasing concentrations of KCl up to 34.05 mM. The % of hypochromicity in the absorption maxima of **4b** were plotted as a function of the salt concentration.

Spectra deconvolution

UV/Vis absorbance spectra of **4b** in both aggregated and monomeric states were analyzed by fitting each data set to a series of Gaussian curves using a least squares fitting procedure.

Fluorescence displacement assay

Fluorescence displacement assay was performed by titrating the **4b**-*c-MYC* Pu22 binary mixture with increasing concentration of the well-known G4-binders Phen-DC_3 or PDS until no changes on the **4b** fluorescence intensity were observed. ($c_{\mathbf{4b}}$ = 2.5 μM, $c_{c\text{-}MYC\ Pu22}$ = 1.25 μM, $c_{Phen\text{-}DC3}$ = from 0 to 1.5 μM, c_{PDS} = from 0 to 11.8 μM, C_{KCl} = 100 mM, Tris buffer 50.0 mM, pH 7.5 at 25 °C).

Polyacrylamide gel electrophoresis (PAGE)

PAGE was conducted in TBE buffer with 20% native gel and 100 mM KCl. Oligonucleotides were heated at 95 °C for 5 min in the presence of 100 mM KCl and then slowly allowed to reach room temperature overnight. Then, oligonucleotides were loaded on the gel and electrophoresis was run at 80 V for 90 minutes at room temperature. After electrophoresis, the gel was stained with **4b** (5 μM) and later on with Thiazole Orange, TO (5 μM) for 10 minutes and rinsed with TBE buffer. Visualization was performed on a Typhoon 9400 scanner by using an excitation wavelength of 457 nm.

DNA polymerase stop assay

The DNA polymerase stop assay was performed as described previously.[S6] Briefly, reactions containing 40 nM template DNA (G4 or non-G4) annealed to a TET-labeled primer was incubated with 0, 5, 10, 15, 20, 30 and 40 μM **4b** in the presence of 50 mM KCl. Control reactions contained 2% DMSO instead of compound. 0.625 U/uL of Taq-DNA polymerase was used in the reactions. Reactions with Taq-DNA polymerase was incubated for 30 minutes at 50 °C. Samples were run on 10% denatured PAGE. Gels were visualized by Typhoon 9400 scanner and quantified by ImageQuant TL software. Fluorescence signal was normalized relatively to DMSO reaction. The last three bands were assigned to the full-length product. The following oligonucleotide sequences were used:

Primer 5′-3′:

^{TET}-TGAAAACATTATTAATGGCGTCGAGCGTCCG

Pu24T 5′-3′:

ATATATATATTGAGGGTGGTGAGGGTGGGGAAGGATATATATATCGGACGCTCGACGC
CATTAATAATGTTTTCA

Tel-22 5′-3′:

ATATATATATAGGGTTAGGGTTAGGGTTAGGGATATATATATCGGACGCTCGACGCCA
TTAATAATGTTTTCA

NonG4 5′-3′:

GAGACCATTCAAAAGGATAATGTTTGTCATTTAGTATATGCCCCTGCTCGTCTTCCCTT
CTCCGGACGCTCGACGCCATTAATAATGTTTTCA

Fluorescence microscopy

HeLa cells (cervical cancer cell line, a kind gift from Dr. Sjoerd Wanrooij's laboratory, Umeå University) were cultured at 37 °C in 5% CO_2 in DMEM high glucose medium (Gibco) supplemented by 10% fetal bovine serum and penicilin-streptomycin. For fixed cell imaging, cells were fixed with 2% paraformaldehyde for 10 min, permeabilized with PBST (phosphate buffer saline supplemented by 0.1% TritonX-100). Fixed cells were treated with **4b** (20 μM) for 30 min at room temperature. For RNA degradation, 0.1 mg/ml RNase A (Thermo Fisher) was used and samples were incubated for 2 hours at 37 °C. For fluorescence competition assay **4b** (20 μM) was incubated with BRACO-19 (20 μM) for 30 min at room temperature. For TMPyP4 studies cells were treated with TMPyP4 (10 μM) alone or with **4b** (60 μM) at room temperature. Images were

acquired by confocal microscope Leica SP8 FALCON (FAst Life time CONtrast) using HC PL APO 63x/1.20 Water motCORR CS2 objective. Maximum intensity projection of Z-stack images was used for data presentation to preserve raw fluorescence signal. All data were processed by using ImageJ software available at https://imagej.nih.gov/ij/.

Nuclear magnetic resonance

The G4 DNA stock solutions was prepared by folding 100 µM *c-MYC* Pu22 in 10 mM potassium phosphate buffer (pH = 7.4) and 35 mM KCl by heating to 95 °C and slowly cooling to room temperature overnight. 10% D_2O and 10% DMSO-d6 was added to the DNA stock solutions, yielding a final DNA concentration of 82 µM. NMR samples were prepared by sequential addition of **4b** from 10 mM DMSO stock solutions to 200 µL of the DNA solution in a 3 mm NMR tube. Control samples with *c-MYC* Pu22 with and without 10% DMSO was also performed to verify that DMSO did not have a significant effect on the DNA structure. All spectra were recorded at 298 K on a Bruker 850 MHz Avance III HD spectrometer equipped with a 5 mm TCI cryoprobe. Excitation sculpting was used in the 1D 1H experiments, and 256 scans were recorded. Processing was performed in Topspin 3.6 (Bruker Biospin, Germany).

Optical studies of 4b

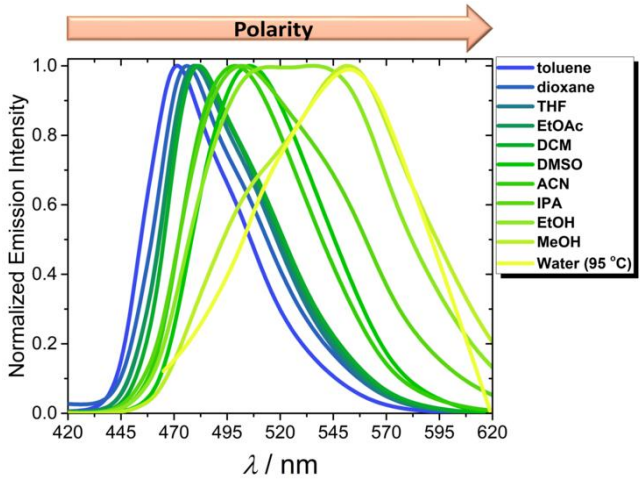

Figure S1. Comparison of polarity-dependent band shifts of **4b** (2.0 µM).

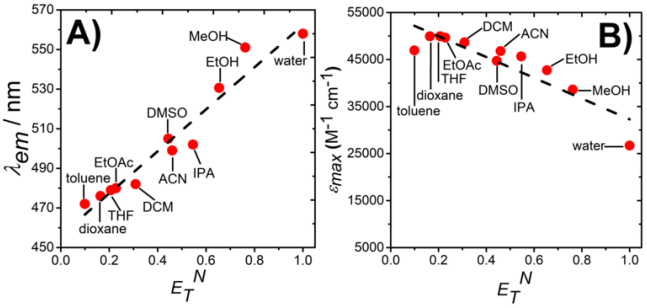

Figure S2. A) Changes of the emission maxima and **B)** extinction coefficient of **4b** depending on the solvent polarity. The values of emission maximum and extinction coefficient in water (ε_{max} = $2.67 \cdot 10^4$ M^{-1} cm^{-1}) are referred to the monomeric state of **4b** originated at 95 °C.

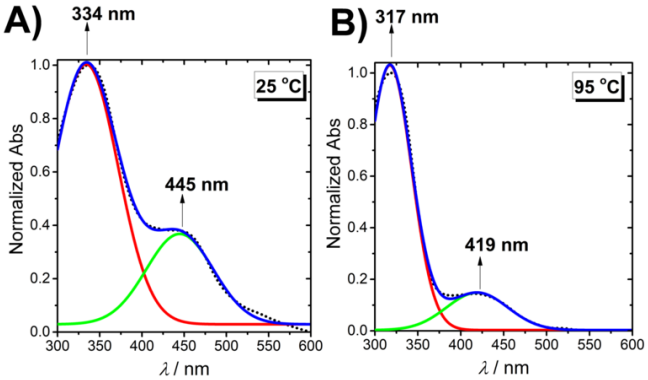

Figure S3. Peak fitting performed on the UV/Vis spectra using a Gaussian curve and a least squares fitting procedure for **4b** at **A)** 25 and **B)** 95 °C ($C_{\mathbf{4b}}$ = 15 µM, C_{KCl} = 100 mM, TRIS buffer 10.0 mM, pH = 7.5). Black dotted lines correspond to the experimental data, red and green lines correspond to the transitions obtained using a Gaussian curve and a least squares fitting procedure and the blue line corresponds to the global fitting.

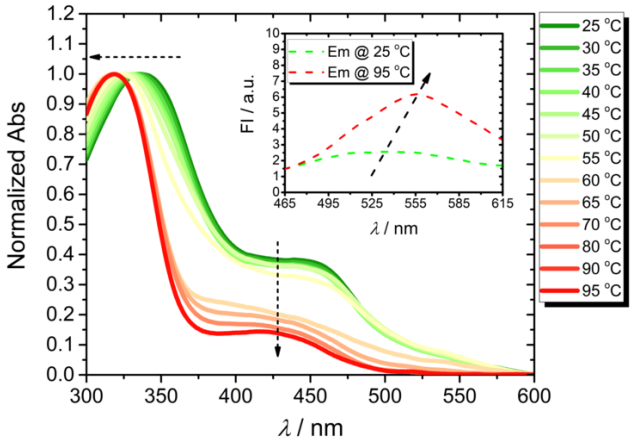

Figure S4. UV/Vis spectrum of a buffered **4b** solution (15.0 µM, C_{KCl} = 100 mM, TRIS buffer 10.0 mM, pH 7.5) upon increasing the temperature from 25 (green) to 95 °C (red). Inset: Plot of the **4b** emission intensity at 25 and 95 °C.

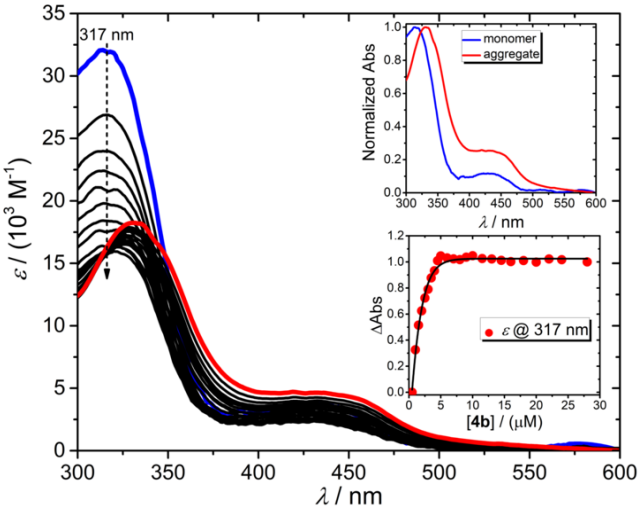

Figure S5. Concentration-dependent UV/Vis studies of **4b** in a water:MeOH (90:10) binary mixture. The **4b** monomer-to-aggregate transition is depicted by the blue (diluted **4b** solution) and red (concentrated **4b** solution) lines (Inset, upper panel). Changes on the extinction coefficient at 317 nm plotted as function of **4b** concentration enable to determine the **4b** aggregation constant (Inset, lower panel). Experimental data were fitted by using the isodesmic model.

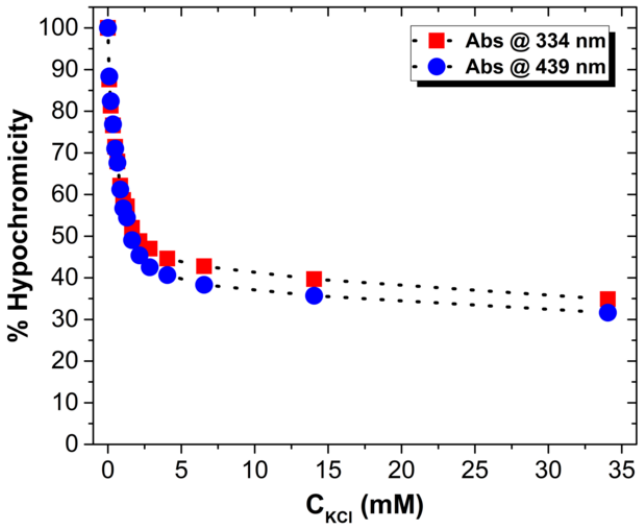

Figure S6. Ionic strength dependence absorption studies of **4b** (15 µM) at increasing KCl concentration (C_{KCl} = 0 to 34.05 mM). The % of hypochromicity reflects the changes of the asborption bands at 334 and 439 nm.

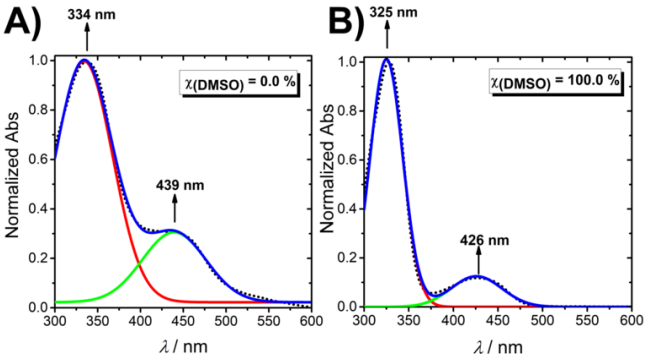

Figure S7. Peak fitting performed on the UV/Vis spectra using a Gaussian curve and a least squares fitting procedure for **4b** (15 µM) in **A)** water and **B)** DMSO. Black dotted lines correspond to the experimental data, red and green lines correspond to the transitions obtained using a Gaussian curve and a least squares fitting procedure and the blue line corresponds to the global fitting.

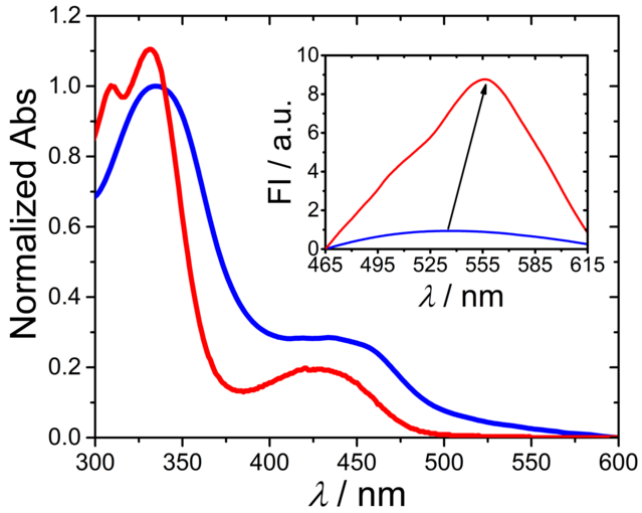

Figure S8. UV/vis spectral changes of a **4b** buffered solution in the absence (blue line) and presence (red line) of SDS (15.0 µM, TRIS buffer 10.0 mM, pH 7.5). Inset: Emission spectral changes of a **4b** buffered solution in the absence (blue line) and presence (red line) of SDS (2.5 µM, TRIS buffer 10.0 mM, pH 7.5).

G4 characterization

Oligonucleotide annealing and morphological characterization

Oligonucleotides were heated at 95 °C for 5 min in the presence of 100 mM KCl and then slowly allowed to reach room temperature overnight. The list of the oligonucleotides used in this study is provided in Table S1.

Table S1. List of the biologically relevant natural and synthetic oligonucleotides.

Name	Sequence[a]	Length (bp)	Molar extinction coefficient ($M^{-1}cm^{-1}$)[b]	GC%	Topology and description
***c-MYC* Pu22 mut**	TGAGGGTGGGTAGGGTGGGTGA	22	226000	63.6	parallel
***c-MYC* Pu22**	TGAGGGTGGGTAGGGTGGGTAA	22	228700	59.1	parallel
***c-MYC* sG4**	GGGTGGGTAGGGTGGG	16	162700	75	parallel
***c-MYC* Pu24T**	TGAGGGTGGTGAGGGTGGGGAAGG	24	248200	66.7	parallel
5′-Texas red-*c-MYC* Pu22	Txred-TGAGGGTGGGTAGGGTGGGTAA	22	228700	59.1	parallel
***c-MYC* Pu22-Texas red-3′**	TGAGGGTGGGTAGGGTGGGTAA-Txred	22	228700	59.1	parallel
bcl-2	GGGCGCGGGAGGGAATTGGCGGGG	24	237400	79.2	parallel
Ceb25	AGGGTGGGTGTAAGTGTGGGTGGGT	25	253100	60	parallel
VEGF	GGGAGGGTTGGGGTGGG	17	171400	76.5	parallel
TG5T	TGGGGGT	7	67900	71.4	parallel
c-kit 2	CCCGGGCGGGCGCGAGGGAGGGGAGG	26	253400	88.5	parallel (snap-back)
c-kit 87up	AGGGAGGGCGCTGGGAGGAGGG	22	226700	77.3	parallel (snap-back)
Tel-22	AGGGTTAGGGTTAGGGTTAGGG	22	228500	54.5	hybrid/anti-parallel
Bom17	GGTTAGGTTAGGTTAGG	17	174600	47.1	anti-parallel
TBA	GGTTGGTGTGGTTGG	15	143300	60	anti-parallel
TGA-ssDNA	GGATGTGAGTGTGAGTGTGAGG	22	227000	54.5	single stranded
dsDNA[c]	/	~2000	13200	/	double stranded

[a] Conventional 5' to 3' direction. [b] Molar extinction coefficient calculated by using oligo analyzer on the IDT web site. [c] Salmon sperm DNA.

Evidences for most of the G4 folding sequences used in this study were provided by ECD measurements and isothermal difference spectra (IDS) defined as the difference between unfolded and prefolded UV/Vis spectra following previously published reports.[S7,S8] ECD spectra were normalized to $\Delta\varepsilon$ ($M^{-1}\cdot cm^{-1}$) = θ / (32980 · c ·l) based on G-quadruplex strand concentration, where θ is the ECD ellipticity in millidegrees, c is DNA concentration in mol/L, and l is the path length in cm.

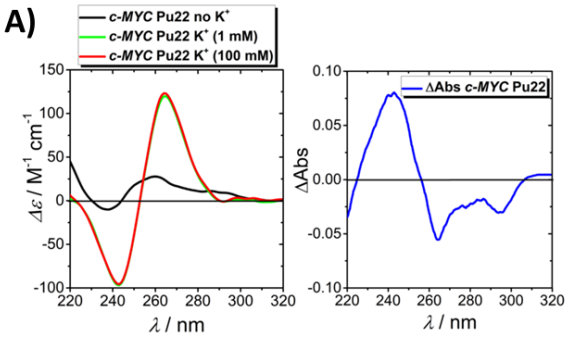
A)
c-MYC Pu22 no K+
c-MYC Pu22 K+ (1 mM)
c-MYC Pu22 K+ (100 mM)
ΔAbs c-MYC Pu22
Δε / M-1 cm-1
ΔAbs
λ / nm

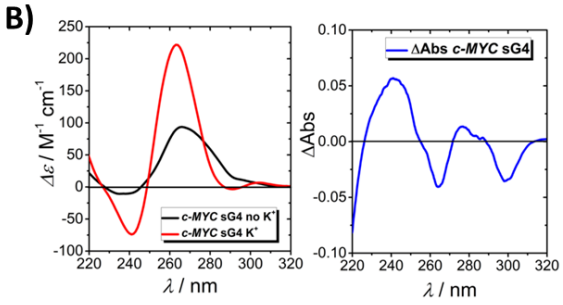
B)
c-MYC sG4 no K+
c-MYC sG4 K+
ΔAbs c-MYC sG4
Δε / M-1 cm-1
ΔAbs
λ / nm

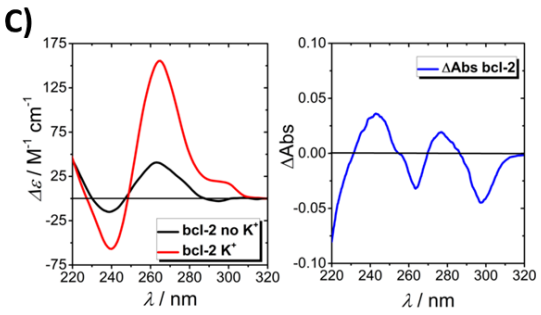
C)
bcl-2 no K+
bcl-2 K+
ΔAbs bcl-2
Δε / M-1 cm-1
ΔAbs
λ / nm

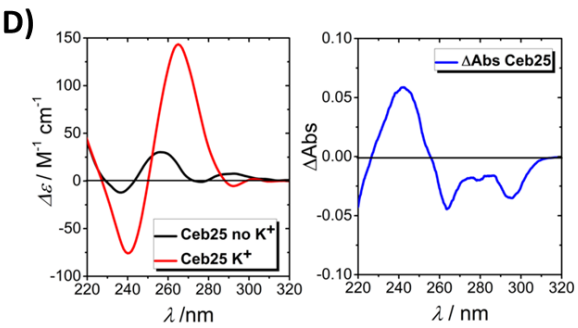
D)
Ceb25 no K+
Ceb25 K+
ΔAbs Ceb25
Δε / M-1 cm-1
ΔAbs
λ /nm

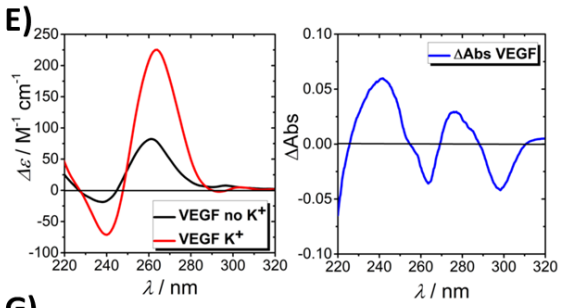
E)
VEGF no K+
VEGF K+
ΔAbs VEGF
Δε / M-1 cm-1
ΔAbs
λ / nm

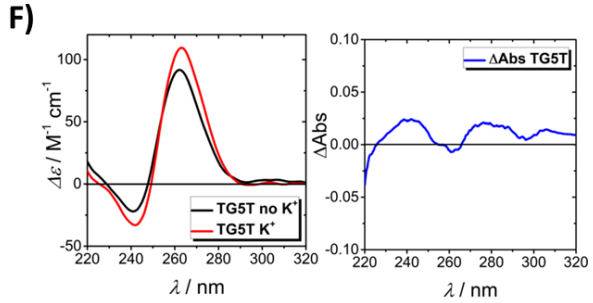
F)
TG5T no K+
TG5T K+
ΔAbs TG5T
Δε / M-1 cm-1
ΔAbs
λ / nm

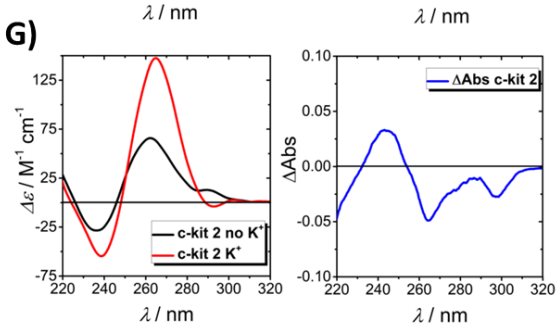
G)
c-kit 2 no K+
c-kit 2 K+
ΔAbs c-kit 2
Δε / M-1 cm-1
ΔAbs
λ / nm

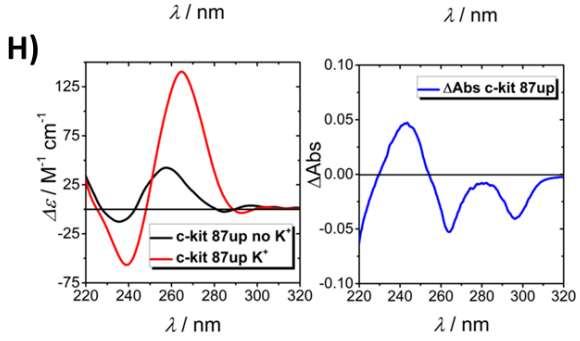
H)
c-kit 87up no K+
c-kit 87up K+
ΔAbs c-kit 87up
Δε / M-1 cm-1
ΔAbs
λ / nm

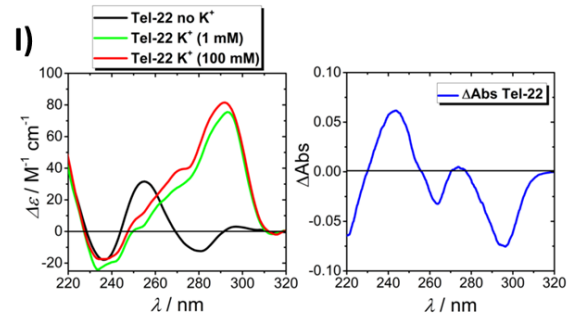
I)
Tel-22 no K+
Tel-22 K+ (1 mM)
Tel-22 K+ (100 mM)
ΔAbs Tel-22
Δε / M-1 cm-1
ΔAbs
λ / nm

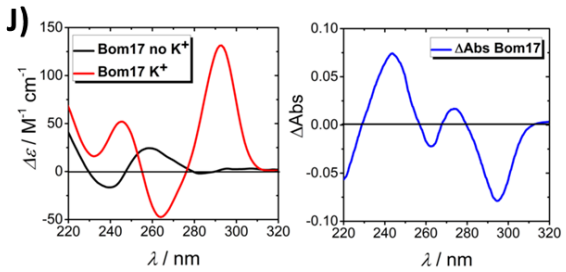
J)
Bom17 no K+
Bom17 K+
ΔAbs Bom17
Δε / M-1 cm-1
ΔAbs
λ / nm

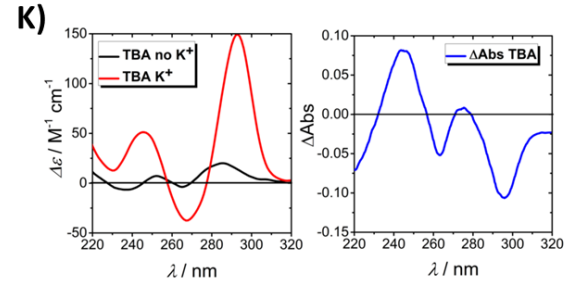
K)
TBA no K+
TBA K+
ΔAbs TBA
Δε / M-1 cm-1
ΔAbs
λ / nm

Figure S9. ECD spectra (black lines: in the absence of K^+; green lines in the presence of 1mM K^+ (only in S9A and S9I), and red lines in the presence of 100 mM K^+) and IDS spectra (blue lines) of **A)** *c-MYC* Pu22, **B)** *c-MYC* sG4, **C)** bcl-2, **D)** Ceb25, **E)** VEGF, **F)** TG5T, **G)** c-kit, **H)** c-kit 87up, **I)** Tel-22, **J)** Bom17, **K)** TBA. All measurements were performed in TRIS buffer 10.0 mM, pH 7.5 at 25 °C.

G4-binding studies

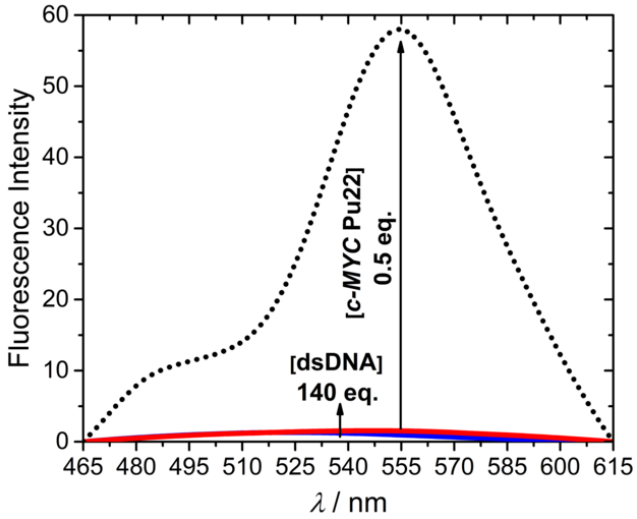

Figure S10. Fluorimetric titration of **4b** in the presence of dsDNA (blue and red lines correspond to the spectra before and after the addition of 140 eq. of dsDNA, respectively). Short dotted line corresponds to the fluorescence enhancement obtained upon addition of 0.5 eq. of *c-MYC* Pu22 to the same solution (C_{KCl} = 100 mM, TRIS buffer 10.0 mM, pH 7.5).

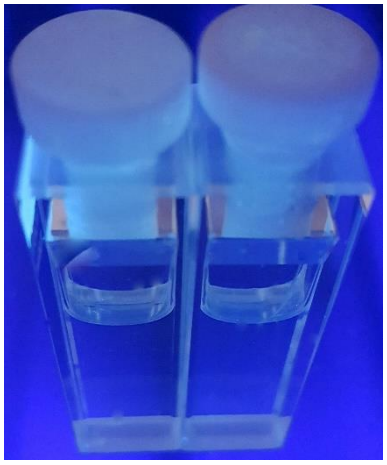

Figure S11. No color changes were observed by the addition of *c-MYC* Pu22 to **4a**. Left cuvette **4a** alone and right cuvette **4a**-*c-MYC* Pu22 mixture ($C_{\mathbf{4a}}$ = 2.5 μM, $C_{c\text{-}MYC\ Pu22}$ = 20 μM, C_{KCl} = 100 mM, TRIS buffer 10.0 mM, pH 7.5).

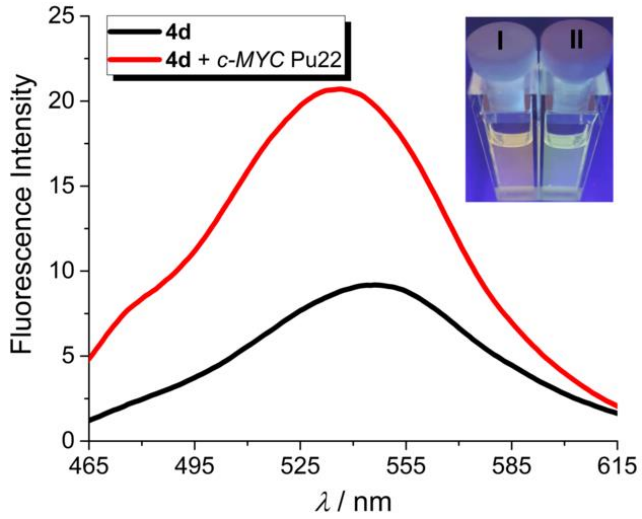

Figure S12. The addition of *c-MYC* Pu22 to **4d** blue-shifted its emission maximum resulting in a clear color change of the solution ($C_{\mathbf{4d}}$ = 2.5 μM, $C_{c\text{-}MYC\ Pu22}$ = 2.5 μM, C_{KCl} = 100 mM, TRIS buffer 10.0 mM, pH 7.5). Left cuvette (I) **4d** alone and right cuvette (II) **4d**-*c-MYC* Pu22 mixture.

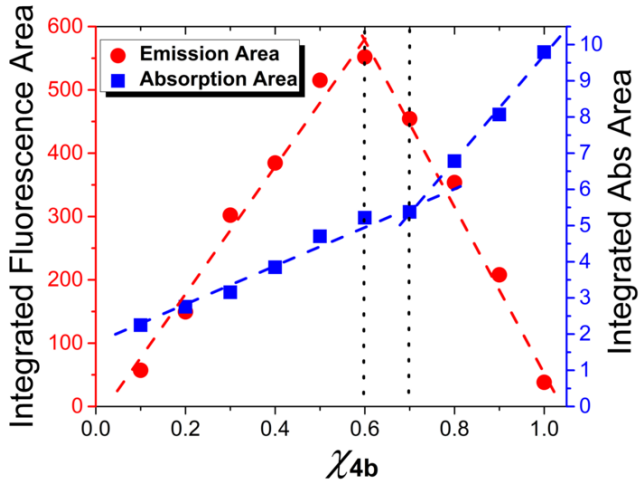

Figure S13. Job's plot for the titration of **4b** with *c-MYC* Pu22 obtained by plotting the integrated emission (red circles) and absorption (blue squares) areas in the range 485-585 and 300-600 nm, respectively. The vertical dotted lines aimed to show the inflection point supporting the 2:1 binding stoichiometry.

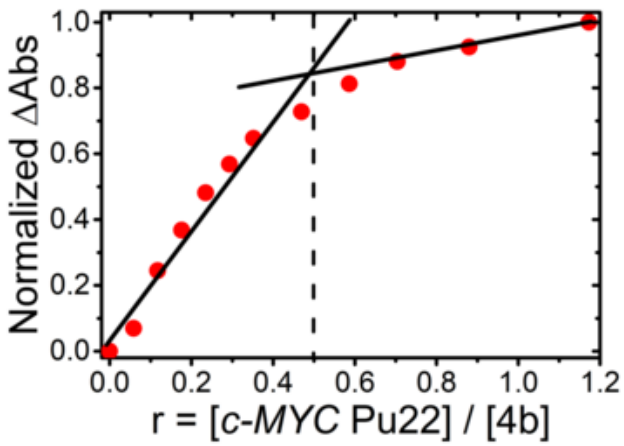

Figure S14. Mole ratio plot for the titration of **4b** with *c-MYC* Pu22 obtained by plotting the absorbance changes at 334 nm. The vertical dotted lines aimed to show the inflection point supporting the 2:1 binding stoichiometry.

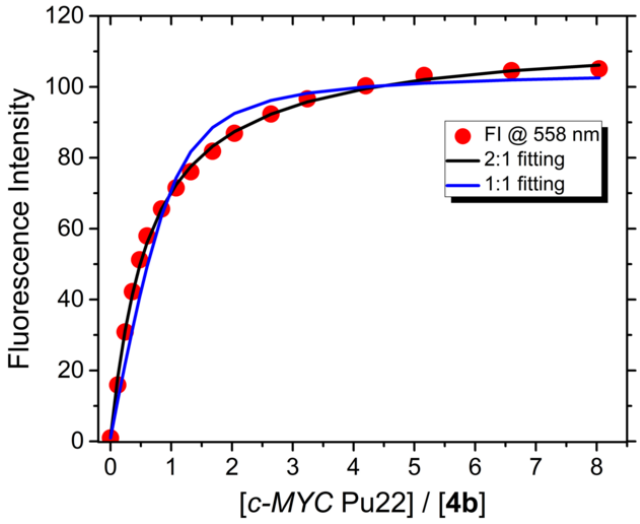

Figure S15. Fluorimetric binding isotherms of **4b** in the presence of *c-MYC* Pu22 ($c_{\mathbf{4b}}$ = 2.5 µM, TRIS buffer (10 mM), pH = 7.5, KCl (100 mM), T = 25 °C, λ_{exc} = 320 nm). The blue and black curves result from a global fitting by using a 1:1 and 2:1 binding stoichiometry, respectively.

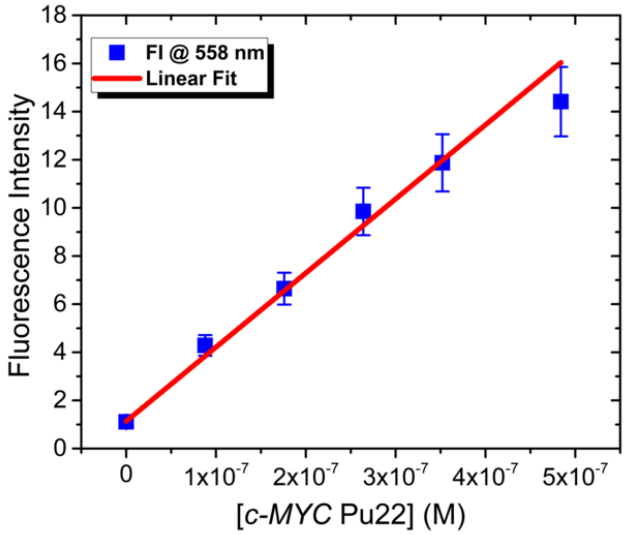

Figure S16. Analysis of the sensitivity of **4b** in detecting *c-MYC* Pu22. The *c-MYC* Pu22 concentration varied between 0.088 and 0.48 µM. 15 measurements were performed on the compounds alone, in order to obtain a reasonable S_b value to use in the LOD calculation. LOD = 49 nM.

Dissociation model of 4b aggregates

The mechanism of interaction of **4b** with *c-MYC* Pu22 was investigated by using the following dissociation model:[S9]

$$\boldsymbol{4b}_n + c - MYC\ Pu22 \underset{k_{off}}{\overset{k_{on}}{\leftrightarrow}} \boldsymbol{4b}_{n-1} + \boldsymbol{4b}{:}\, c - MYC\ Pu22 \qquad (Eq.S5)$$

where **4b**$_n$, *c-MYC* Pu22 and **4b**:*c-MYC* Pu22 represent the **4b** aggregate, the G4 structure and the complex of **4b** with *c-MYC* Pu22, respectively. Such a model would predict an increase in the apparent rate constant of dissociation of the **4b** aggregate with an increase in concentration of *c-MYC* Pu22. As shown in Figure S17, the apparent rate constant increased with increasing *c-MYC* Pu22 concentration indicating that the G4 structure binds and catalyzes dissociation of **4b** molecular aggregates.

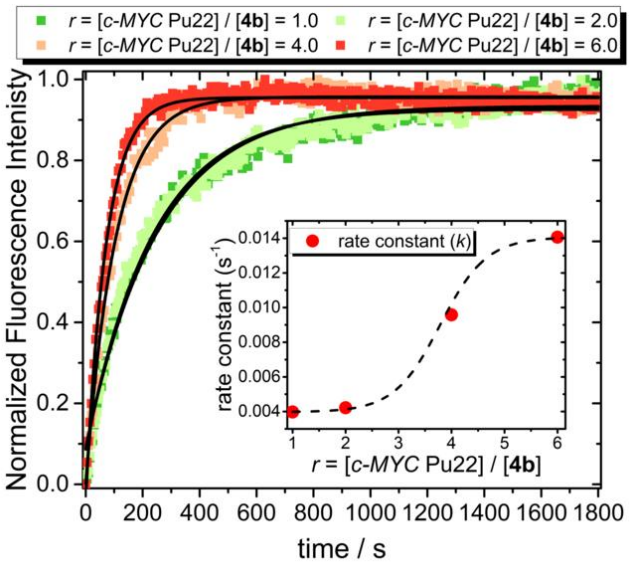

Figure S17. Effect of increasing concentration of *c-MYC* Pu22 on the dissociation kinetics of **4b** aggregates. Apparent rate constant (*k*) was obtained by fitting the kinetic data to a monoexponential function.

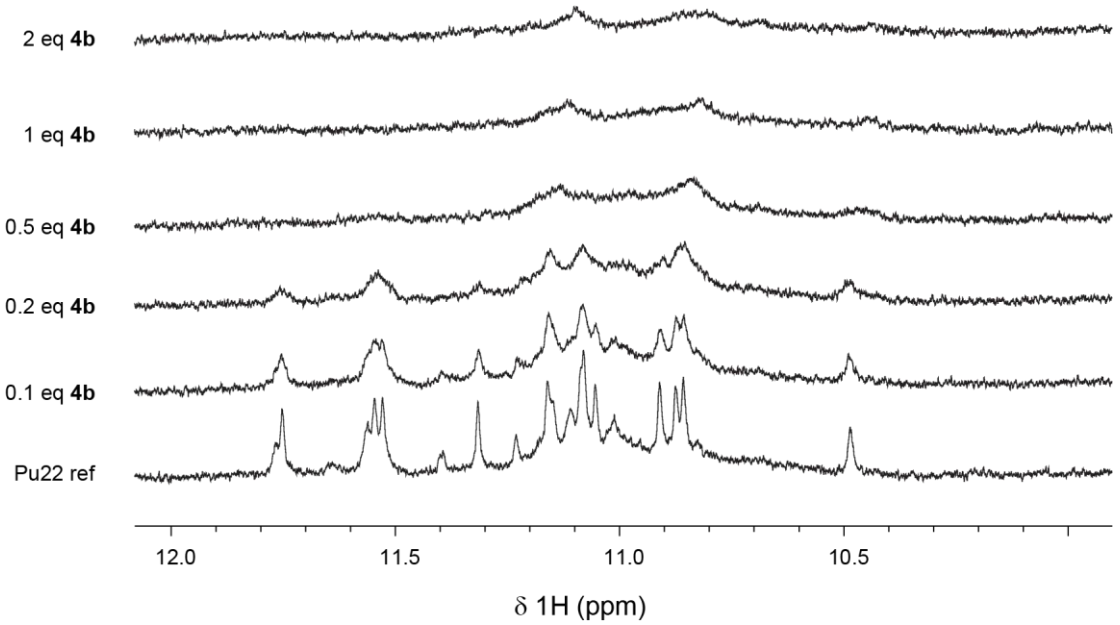

Figure S18. NMR spectra showing the imino-region of *c-MYC* Pu22 in presence of different amount of **4b** (0.0:1, 0.1:1, 0.2:1, 0.5:1, 1:1, 2:1, compound:G4 DNA).

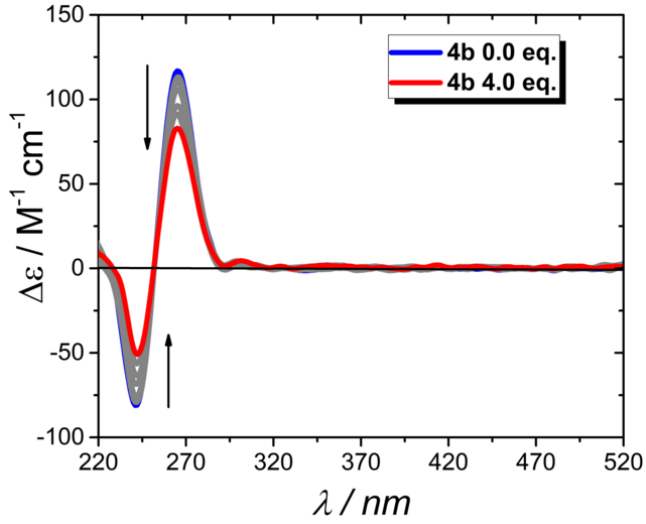

Figure S19. ECD spectra of *c-MYC* Pu22 upon addition of **4b** (blue and red lines correspond to the spectra at 0.0 eq. and 4.0 eq., respectively). Experimental conditions: TRIS buffer 10.0 mM, pH 7.5, KCl 100 mM, 25 °C.

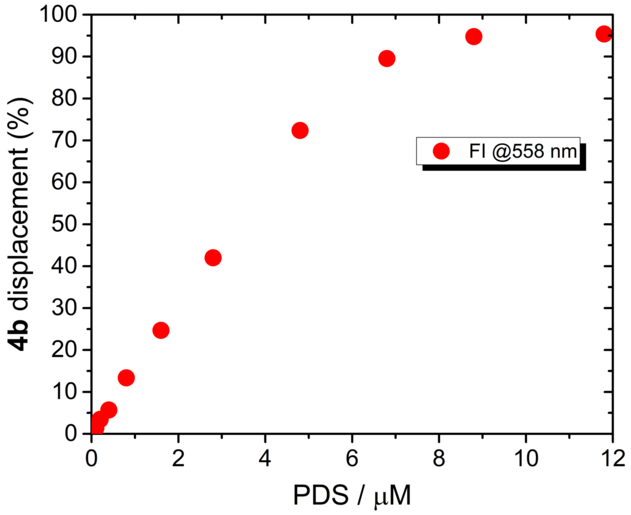

Figure S20. Fluorescence emission changes on the **4b**-*c-MYC* Pu22 system upon increasing concentration of Pyridostatin (**4b** = 2.5 μM, *c-MYC* Pu22 = 1.25 μM and Pyridostatin concentration ranged from 0 to 11.8 μM). Experimental conditions: TRIS buffer 10.0 mM, pH 7.5, KCl 100 mM, 25 °C.

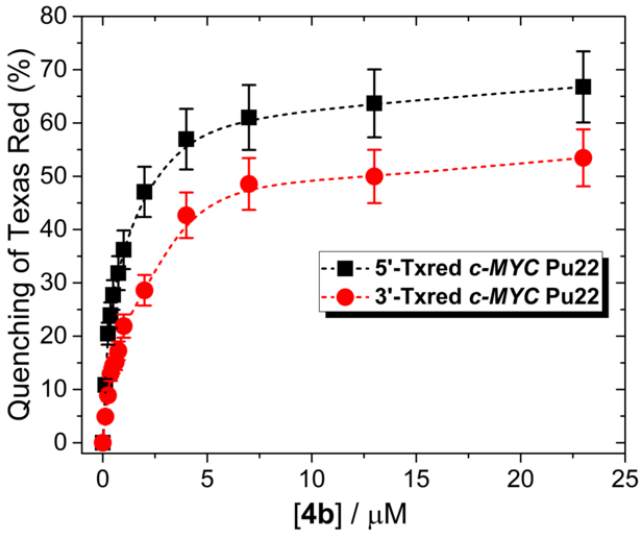

Figure S21. G-tetrad selectivity analysis of 5′- (black squares) and 3′- (red circles) Texas red labelled *c-MYC* Pu22 upon titration with **4b**. [5′-Txred *c-MYC* Pu22] = [3′-Txred *c-MYC* Pu22] = 0.25 μM. Short dashed lines aimed only to guide the eyes.

Photophysical data for 4b-*c-MYC* G4 systems

Table S2. Photophysical data for **4b**-*c-MYC* G4 systems.

Systems	τ_1 (ns)	τ_2 (ns)	τ_3 (ns)	A_1(%)	A_2(%)	A_3(%)	<τ> (ns)
4b-*c-MYC* Pu22 mut	1.00	3.56	13.29	90.1	6.5	3.4	4.90
4b-*c-MYC* Pu22	0.91	3.22	13.23	91.7	5.7	2.6	4.37
4b-*c-MYC* Pu24T	3.08	0.98	14.01	6.4	91.8	1.8	3.67
4b-*c-MYC* sG4	2.80	0.79	14.82	3.9	95.5	0.6	2.39

τ_1, τ_2 and τ_3: lifetime decay components, A_1, A_2 and A_3: relative amplitudes with their sum normalized to unity, <τ>: average lifetime.

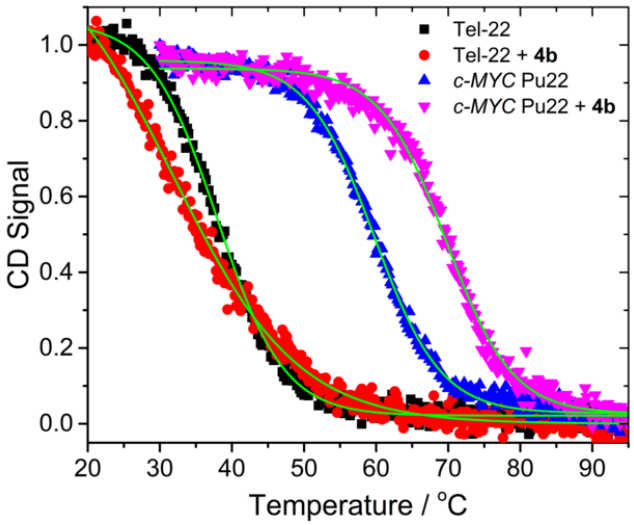

Figure S22. CD melting of *c-MYC* Pu22 and Tel-22 in the presence of **4b** (*c-MYC* Pu22 = 2.0 μM, Tel-22 = 2.0 μM, **4b** = 10 μM, KCl = 1 mM).

Synthesis

Experimental procedure

General:

All analytical grade reagents and solvents were purchased from either Sigma-Aldrich, Fluka, or Acros and used as supplied unless stated otherwise. Thin layer chromatography (TLC) was used for monitoring of chemical reactions and performed on aluminium backed silica gel plates (median pore size 60 Å, fluorescent indicator 254 nm) and detected with UV light. Dimethylformamide (DMF) was dried in a solvent drying system (activated molecular sieves in combination with an isocyanate scrubber). ^{1}H and ^{13}C NMR spectra were recorded on Bruker 400 or 600 MHz spectrometers at 298 K and calibrated by using the residual peak of the solvents as the internal standard (DMSO-d_6 : δ H = 2.50 ppm; δ C = 39.50 ppm; $CDCl_3$: δ H = 7.26 ppm; δ C = 77.02 ppm and acetone-d_6 : δ H = 2.05 ppm; C = 29.82 & 206.03). The coupling constant values (*J*) are determined in Hertz. The abbreviations used in NMR data are mentioned as, broad singlet = brs, singlet = s, doublet = d, triplet = t, multiplet = m, and double doublet = dd. LC-MS was conducted on an Agilent 6150 Series Quadrupole LC/MS system. HRMS was performed by using a Agilent 1290 binary LC System connected to a Agilent 6230 Accurate-Mass TOF LC/MS (ESI+); calibrated with Agilent G1969-85001 ESTOF Reference Mix containing ammonium trifluoroacetate, purine and hexakis (1H, 1H, 3Htetrafluoropropoxy)phosphazine in 90:10 acetonitrile:water.

General procedure for the synthesis of 2,2,4-trimethyl-1,2-dihydroquinoline derivatives 2(a-c): To the mixture of anilines **1**(**a-c**) (12.17 mmol) and anhydrous magnesium sulphate (60.85 mmol) in anhydrous acetone (50 ml) was added iodine (5 mol%) and *tert*-butylcatechol (3 mol%) before being heated to reflux for 24 h. The progress of the reaction was monitored by TLC. Upon consumption of aniline, the reaction mixture was allowed to cool and filtered through a bed of celite. The filtrate solution so obtained was concentrated under reduced pressure to give a brown colored semi-solid material which was purified through column chromatography over silica in 0-0.5% ethylacetate-heptane to give the desired 2,4-trimethyl-1,2-dihydroquinoline derivatives **2**(**a-c**).

2,2,4-Trimethyl-1,2-dihydroquinoline (**2a**): The title compound (**2a**) was obtained from the reaction of aniline (**1a**) with acetone as a brown oil in 68% yield by following the general procedure. ^{1}H NMR (400 MHz, $CDCl_3$), δ (ppm): 7.07 (d, *J* = 4.0 Hz, 1H), 6.99 (t, *J* = 8.0 Hz, 1H), 6.65 (t, *J* = 8.0 Hz, 1H), 6.45 (d, *J* = 4.0 Hz, 1H), 5.32 (s, 1H), 2.00 (s, 3H), 1.29 (s, 6H); ^{13}C NMR (100 MHz, $CDCl_3$), δ (ppm): 143.15, 128.56, 128.37, 128.35, 123.62, 121.59, 117.23, 113.00, 51.84, 31.00, 18.61; ESI MS (m/z): calculated for $C_{12}H_{16}N$ $(M+H)^+$: 174.1277, found 174.3.

***N*,*N*-Diethyl-2,2,4-trimethyl-1,2-dihydroquinolin-6-amine** (**2b**): The title compound (**2b**) was obtained from the reaction of 4-amino-*N*,*N*-diethylaniline (**1b**) with acetone as a brown oil in 57% yield by following the general procedure**.** ^{1}H NMR (400 MHz, $CDCl_3$), δ (ppm): 6.72 (d, *J* = 4.0 Hz, 1H), 6.63 (dd, *J* = 4.0 & 8.0 Hz, 1H), 6.42 (d, *J* = 4.0 Hz, 1H), 5.39 (s, 1H), 3.76 (s, 3H), 2.00 (s, 3H), 1.26 (s, 6H); ^{13}C NMR (100 MHz, $CDCl_3$), δ (ppm): 152.03, 137.53, 129.79, 128.54, 122.98, 113.70, 113.51, 110.10, 55.90, 51.73, 30.36, 18.62; ESI MS (m/z): calculated for $C_{13}H_{18}NO$ $(M+H)^+$: 204.1383, found 204.3.

Benzyl (2,2,4-trimethyl-1,2-dihydroquinolin-6-yl)carbamate (**2c**): The title compound (**2c**) was obtained from the reaction of benzyl (4-aminophenyl)carbamate [(**1c**), first synthesized by reaction of 1,4-diaminebenzene with benzyl chloroformate through a reported procedure[S10], with acetone as a brown oil in 49% yield by following the general procedure. ^{1}H NMR (400 MHz, acetone-*d*$_6$), δ (ppm): 8.25 (brs, 1H), 7.31-7.42 (m, 5H), 7.24 (d, *J* = 8.0 Hz, 1H), 7.11 (d, *J* = 8.0 Hz, 1H), 6.44 (d, *J* = 8.0 Hz, 1H), 5.35 (s, 1H), 5.13 (s, 2H), 4.90 (brs, 1H), 1.92 (s, 3H), 1.23 (s, 6H) ^{13}C NMR (100 MHz, acetone-*d*$_6$), δ (ppm): 153.76, 140.42, 137.41, 129.06, 128.34, 127.99, 127.91, 127.79, 125.73, 121.17, 119.65, 116.27, 114.70, 112.68, 112.58, 65.59, 51.33, 17.83 ESI MS (m/z): calculated for $C_{20}H_{23}N_2O_2^+$ $(M+H)^+$: 323.18, found 323.2.

General procedure for the synthesis of 1-(4-methylquinazolin-2-yl)guanidine derivatives (**3a-c**): To the mixture of 2,2,4-trimethyl-1,2-dihydroquinoline (0.5g, 2.46 mmol) in 1.1 ml of 2M HCl solution, 2-cynoguanidine (0.248 g, 2.95 mmol) was added and the mixture was heated at 100 °C for 0.5 h. The reaction mixture was then cooled to 0-5 °C and basified (until pH 9-10) with a cold 2M solution of NaOH. The process resulted in precipitation, which was collected through filtration and washed with water and diethyl ether to give pure 1-(4-methylquinazolin-2-yl)guanidine derivatives **(3a-c**) in 43-51% yield.

1-(4-Methylquinazolin-2-yl)guanidine (**3a**): The title compound (**3a**) was obtained from the reaction of **2a** with 2-cynoguanidine as a white solid in 51% yield by following the general procedure. ^{1}H NMR (400 MHz, DMSO-*d*$_6$), δ (ppm): 7.97 (d, *J* = 8.0 Hz, 1H), 7.69 (t, *J* = 8.0 Hz, 1H), 7.57 (d, *J* = 8.0 Hz, 1H), 7.49 (brs, 2H), 7.29 (t, *J* = 8.0 Hz, 1H), 2.73 (s, 3H); ^{13}C NMR (100 MHz, DMSO-*d*$_6$), δ (ppm): 169.58, 161.52, 159.30, 150.13, 134.00, 126.29, 125.98, 123.97, 119.89, 22.00; ESI MS (m/z): calcd for $C_{10}H_{12}N_5$ $(M+H)^+$: 202.1087, found 202.2.

1-(6-(Diethylamino)-4-methylquinazolin-2-yl)guanidine (**3b**): The title compound (**3b**) was obtained from the reaction of **2b** with 2-cynoguanidine as a white solid in 43% yield by following the general procedure. ^{1}H NMR (400 MHz, DMSO-*d*$_6$), δ (ppm): 7.97 (d, *J* = 8.0 Hz, 1H), 7.69 (t, *J* = 8.0 Hz, 1H), 7.57 (d, *J* = 8.0 Hz, 1H), 7.49 (brs, 2H), 7.29 (t, *J* = 8.0 Hz, 1H), 2.73 (s, 3H); ^{13}C

NMR (100 MHz, DMSO-d_6), δ (ppm): 169.58, 161.52, 159.30, 150.13, 134.00, 126.29, 125.98, 123.97, 119.89, 22.00; ESI MS (m/z): calcd for $C_{10}H_{12}N_5$ $(M+H)^+$: 202.1087, found 202.2.

Benzyl (2-guanidino-4-methylquinazolin-6-yl)carbamate (**3c**): The title compound (**3c**) was obtained from the reaction of **2c** with 2-cynoguanidine as a white solid in 57% yield by following the general procedure. ^{1}H NMR (400 MHz, DMSO-d_6), δ (ppm): 11.07, (brs, 1H), 10.29 (brs, 1H), 8.44 (brs, 3H), 8.36 (s, 1H), 7.90-7.94 (m, 2H), 7.36-7.47 (m, 5H), 5.21 (s, 2H), 2.82 (s, 3H); ^{13}C NMR (100 MHz, DMSO-d_6), δ (ppm): 171.08, 155.87, 153.97, 152.77, 145.06, 137.56, 136.85, 128.99, 128.87, 128.64, 128.21, 127.89, 121.81, 111.77, 66.59, 21.96; ESI MS (m/z): calcd for $C_{18}H_{19}N_6O_2^+$ $(M+H)^+$: 351.16, found 351.2.

General procedure for the synthesis of 2-((4-methylquinazolin-2-yl)amino)quinazolin-4-ol 4(**a-c**): To the mixture of 1-(4-methylquinazolin-2-yl)guanidine derivatives **3**(**a-c**) (0.38 mmol) and isatoic anhydride (0.46 mmol) in anhydrous DMF (1 mL), diisopropylethylamine (0.46 mmol) was added and the reaction mixture was heated at 100 °C for 12 h. The reaction became a clear solution after stirring for 15 min and reprecipitation of product appeared after 8 hrs. On completion, the reaction mixture was allowed to cool to room temperature for more precipitation. Finally, precipitates so obtained were filtered, washed with methanol, and purified either through crystallization in hot methanol or through column chromatography over silica in 0-2% methanol and 0.5% triethylamine in chloroform to give the desired 2-((4-methylquinazolin-2-yl)amino)quinazolin-4-ol 4(**a-c**) in 51-63% yield.

2-((4-Methylquinazolin-2-yl)amino)quinazolin-4(1*H*)-one (**4a**) (ECH-91): The title compound (**4a**) was obtained from the reaction of **3a** with isatoic anhydride, as a white solid, purified through crystallization in 63% yield by following the general procedure. ^{1}H NMR (400 MHz, DMSO-d_6), δ (ppm): 13.70 (brs, 1H), 11.30 (brs, 1H), 8.24 (d, J = 8.0 Hz, 1H), 8.08 (d, J = 8.0 Hz, 1H), 7.97 (t, J = 8.0 Hz, 1H), 7.80 (d, J = 8.0 Hz, 1H), 7.74 (t, J = 8.0 Hz, 1H), 7.59 (t, J = 8.0 Hz, 1H), 7.48 (d, J = 8.0 Hz, 1H), 7.34 (s, 1H), 2.93 (s, 3H); ^{13}C NMR (150 MHz, DMSO-d_6), δ (ppm): 172.14, 165.01, 155.49, 148.89, 135.65, 134.96, 126.70, 126.62, 126.30, 125.98, 124.17, 120.97, 119.39, 22.01; HRMS: (*m/z*) calcd for $C_{17}H_{14}N_5O$ $[M+H]^+$: 304.1193, found 304.1184.

2-((6-(Diethylamino)-4-methylquinazolin-2-yl)amino)quinazolin-4(1*H*)-one (**4b**) (ECH-106): The title compound (**4b**) was obtained from the reaction of **3b** with isatoic anhydride, as a greenish-yellow solid, purified through column chromatography in 51% yield by following the general procedure. ^{1}H NMR (400 MHz, DMSO-d_6), δ (ppm): 13.73 (brs, 1H), 10.93 (brs, 1H), 8.04 (d, J = 8.0 Hz, 1H), 7.71 (t, J = 8.0 Hz, 1H), 7.62-7.64 (m, 1H), 7.57 (dd, J = 4.0 & 8.0 Hz, 1H), 7.43 (d, J = 8.0 Hz, 1H), 7.29 (t, J = 8.0 Hz, 1H), 6.95 (d, J = 4.0 Hz, 1H), 3.48 (q, J = 8.0 Hz, 4H), 2.82 (s,

3H), 1.16 (t, *J* = 8.0 Hz, 6H); ^{13}C NMR (100 MHz, DMSO-d$_6$), δ (ppm): 168.80, 161.42, 152.28, 150.76, 148.73, 145.55, 140.84, 134.99, 127.12, 126.58, 125.57, 124.31, 123.65, 122.44, 119.06, 102.24, 44.34, 22.13, 12.72; HRMS: (m/z) calcd for $C_{21}H_{23}N_6O^+$ $[M+H]^+$: 375.1928, found 375.1923.

Benzyl(4-methyl-2-((4-oxo-1,4-dihydroquinazolin-2-yl)amino)quinazolin-6-yl)carbamate (**4c**): The title compound (**4c**) was obtained from the reaction of 3c with isatoic anhydride, as yellow solid, purified through crystallization in 57% yield by following the general procedure. ^{1}H NMR (400 MHz, DMSO-d$_6$), δ (ppm): 13.50 (brs, 1H), 10.90 (brs, 1H), 10.06 (s, 1H), 8.33 (s, 1H), 8.07 (d, *J* = 8.0 Hz, 1H), 7.99 (d, *J* = 8.0 Hz, 1H), 7.78 (d, *J* = 8.0 Hz, 1H), 7.72 (t, *J* = 8.0 Hz, 1H), 7.30-7.48 (m, 7H), ^{13}C NMR not recorded due to poor solubility; (HRMS: (m/z): calcd for $C_{25}H_{21}N_6O_3^+$ $(M+H)^+$: 453.1670; found 453.1671.

Synthesis of 2-((6-Amino-4-methylquinazolin-2-yl)amino)quinazolin-4(1*H*)-one (**4d**) (ECH-107): The title compound **4d** was obtained by acidic hydrolysis of benzyl (4-methyl-2-((4-oxo-1,4-dihydroquinazolin-2-yl)amino)quinazolin-6-yl)carbamate (100 mg, 0.221 mmol) with 0.5 mL of acetic acid-HBr (7:3) mixture under refluxing conditions for 12 h. The reaction mixture was then concentrated under reduced pressure, poured into crushed ice, and basified (pH ~ 8-9) to give a brown solid. The brown solid was purified through column chromatography on silica gel by eluting with methanol (0-2%) and triethylamine (0.2%) in DCM to give the desired compound (**4d**) in 66% yield. ^{1}H NMR (400 MHz, DMSO-*d*$_6$), δ (ppm): 13.76 (brs, 1H), 10.91 (brs, 1H), 8.05 (d, *J* = 4.0Hz, 1H), 7.71 (t, *J* = 8.0 Hz, 1H), 7.56 (d, *J* = 8.0 Hz, 1H), 7.43 (d, *J* = 8.0 Hz, 1H),), 7.37 (d, *J* = 8.0 Hz, 1H), 7.29 (t, *J* = 8.0 Hz, 1H), 7.05 (s, 1H), 5.72 (s, 2H), 2.76 (s, 3H); ^{13}C NMR (100 MHz, DMSO-*d*$_6$), δ (ppm): 168.34, 161.43, 152.19, 150.74, 148.78, 147.21, 141.45, 135.00, 127.00, 126.88, 126.99, 126.87, 126.58, 125.56, 123.64, 122.43, 119.05, 103.67, 21.99; HRMS: (m/z): calcd for $C_{17}H_{15}N_6O^+$ $(M+H)^+$: 319.1302; obtained 319.1302.

The existance of three keto-enolic forms of the desired compounds (**4a-d**) are shown in Figure S23.

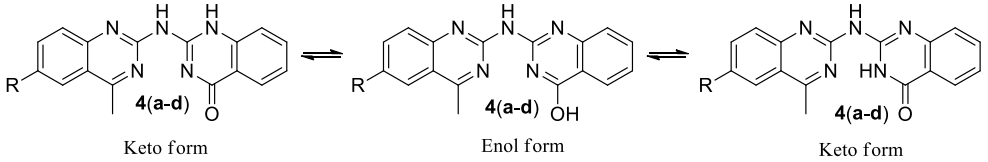

Figure S23. Tautomeric forms for compounds **4a-d**.

NMR Spectra

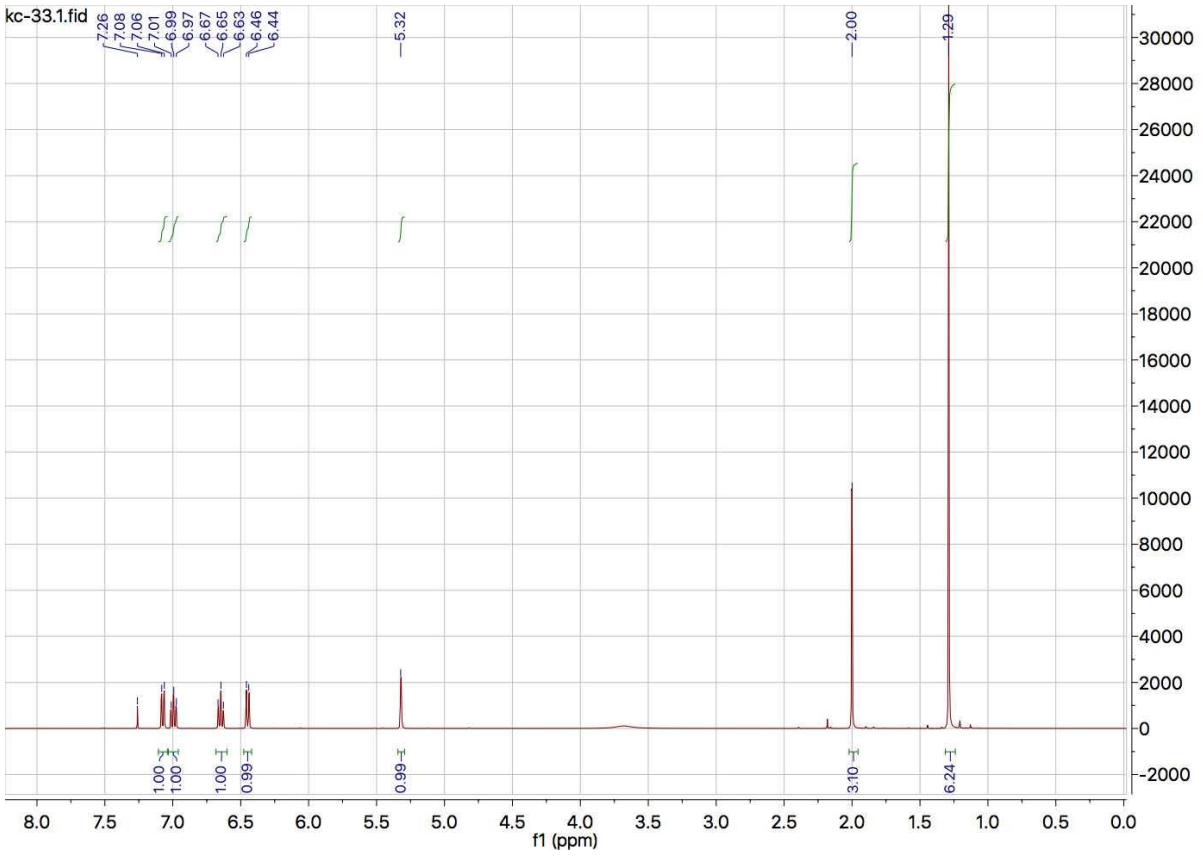

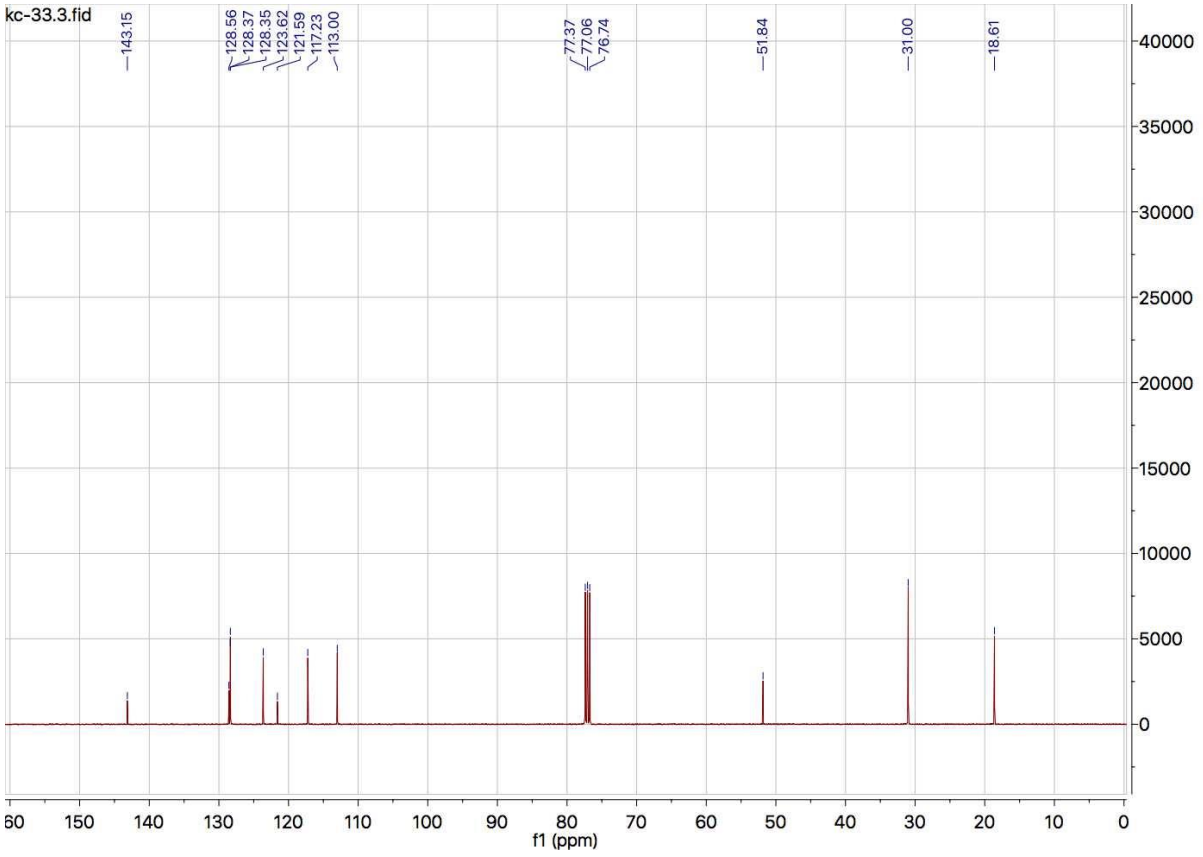

^{1}H and ^{13}C NMR of 2,2,4-Trimethyl-1,2-dihydroquinoline (**2a**).

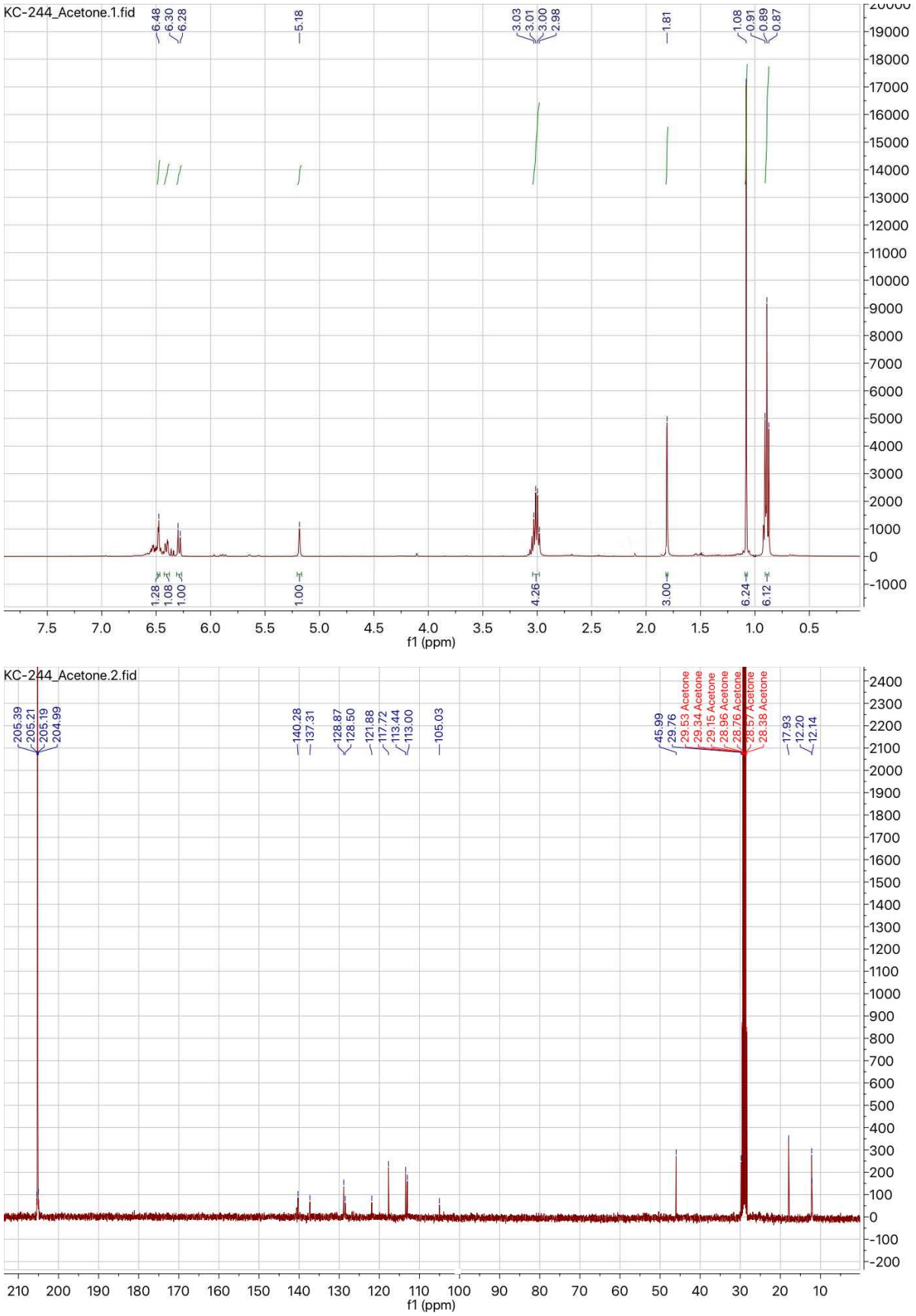

^{1}H and ^{13}C NMR of *N*,*N*-Diethyl-2,2,4-trimethyl-1,2-dihydroquinolin-6-amine (**2b**).

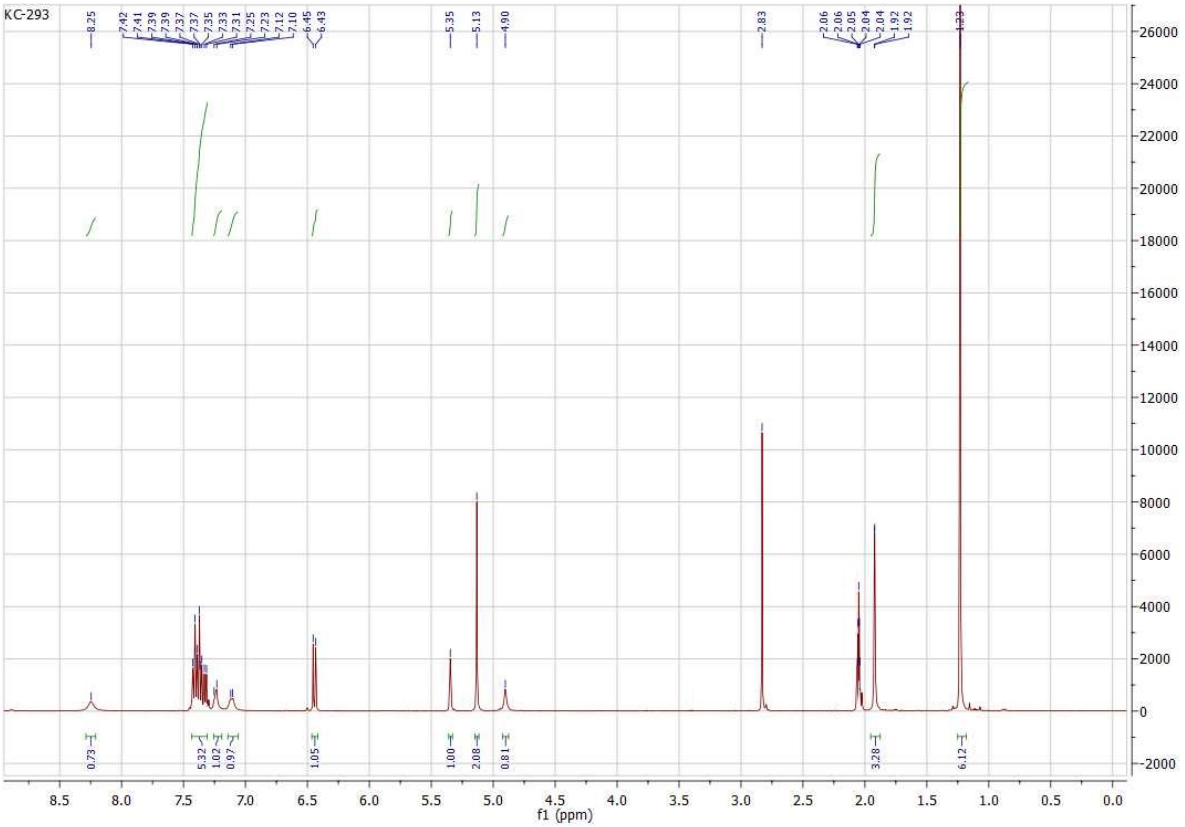

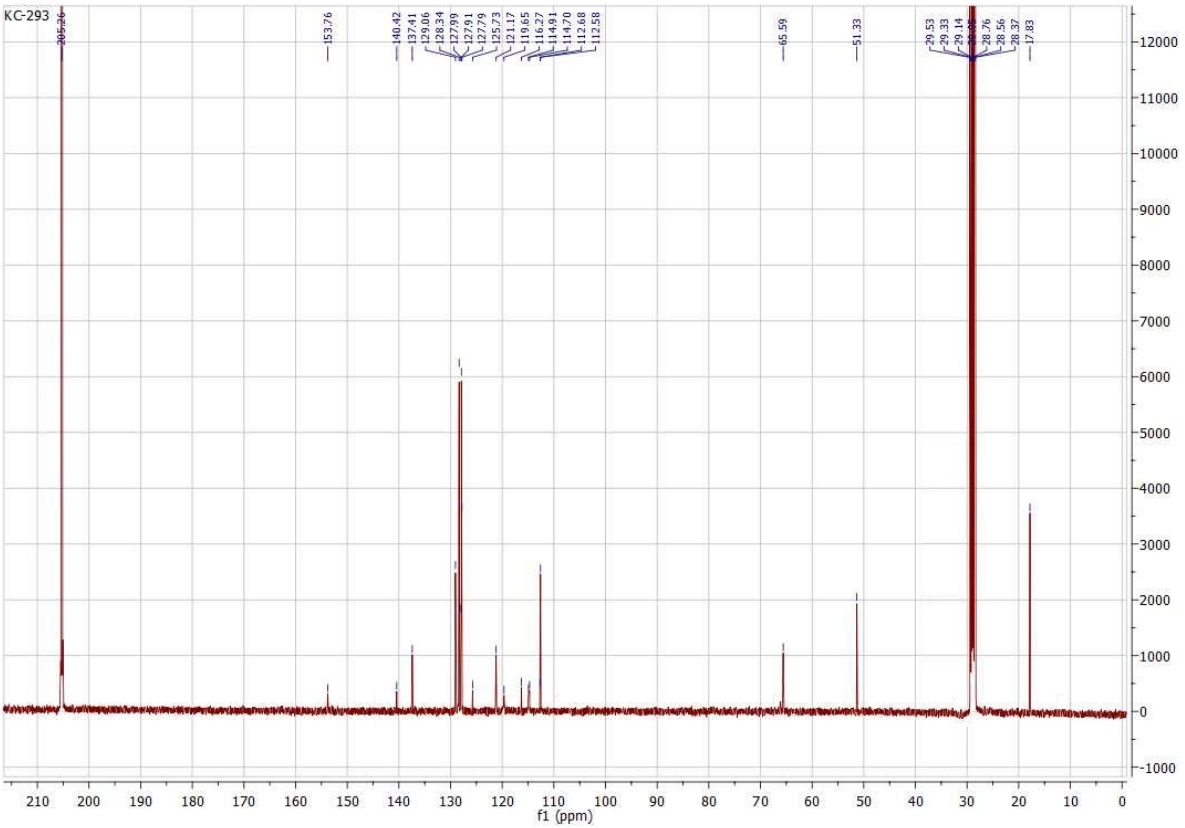

^{1}H and ^{13}C NMR of benzyl (2,2,4-trimethyl-1,2-dihydroquinolin-6-yl)carbamate (**2c**):

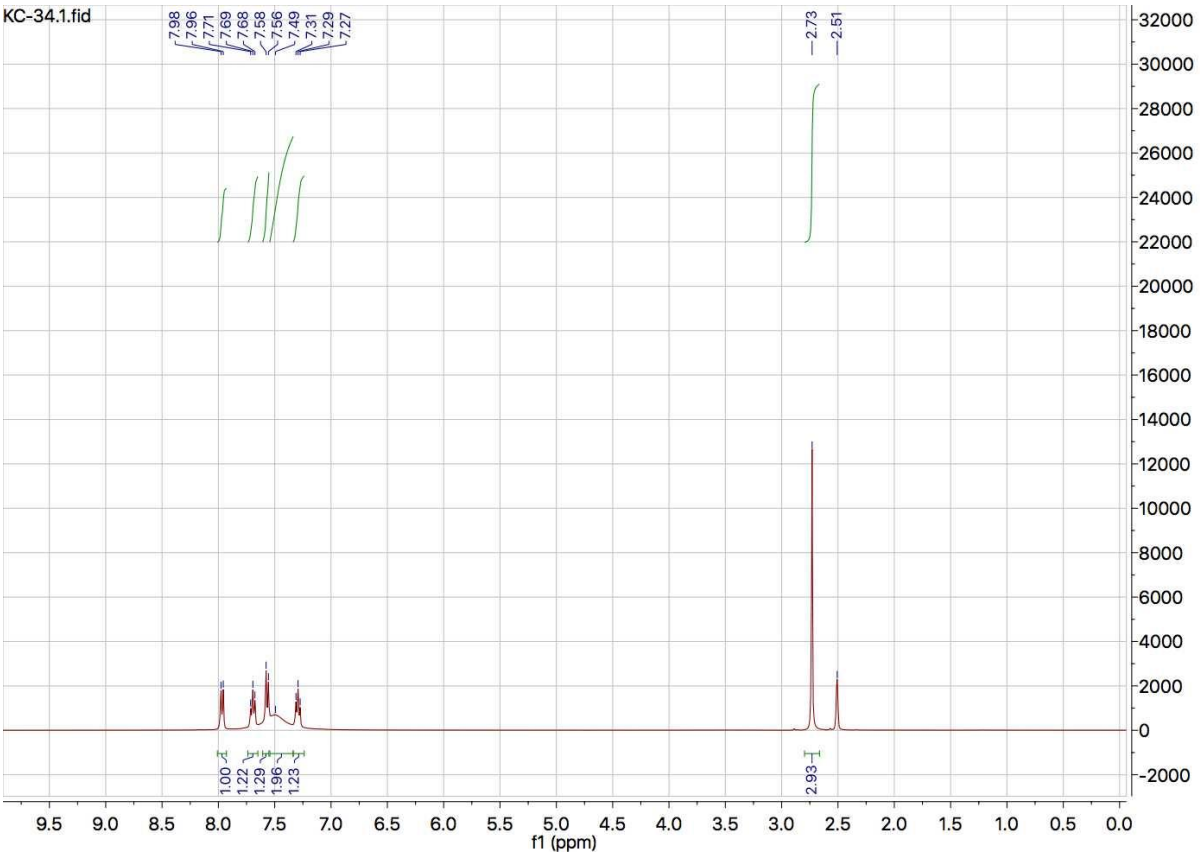

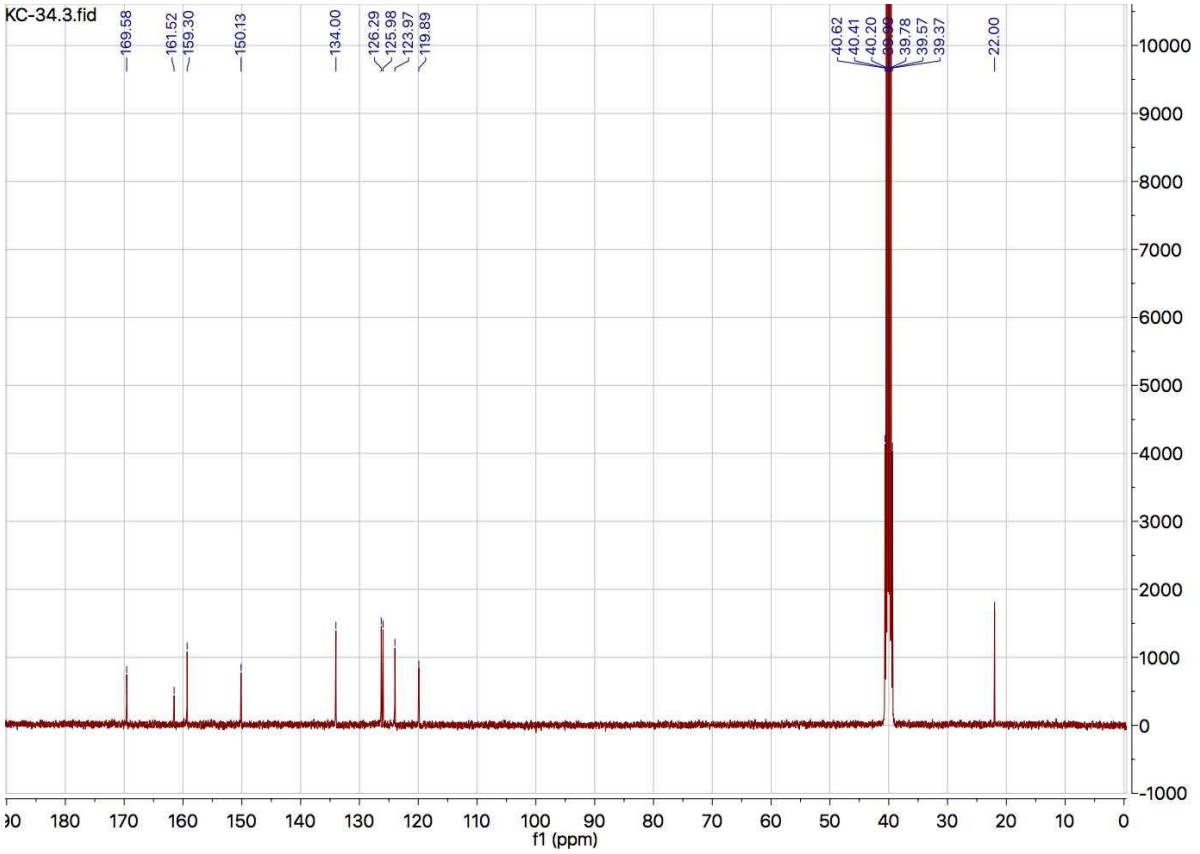

^{1}H and ^{13}C NMR of 1-(4-Methylquinazolin-2-yl)guanidine (**3a**).

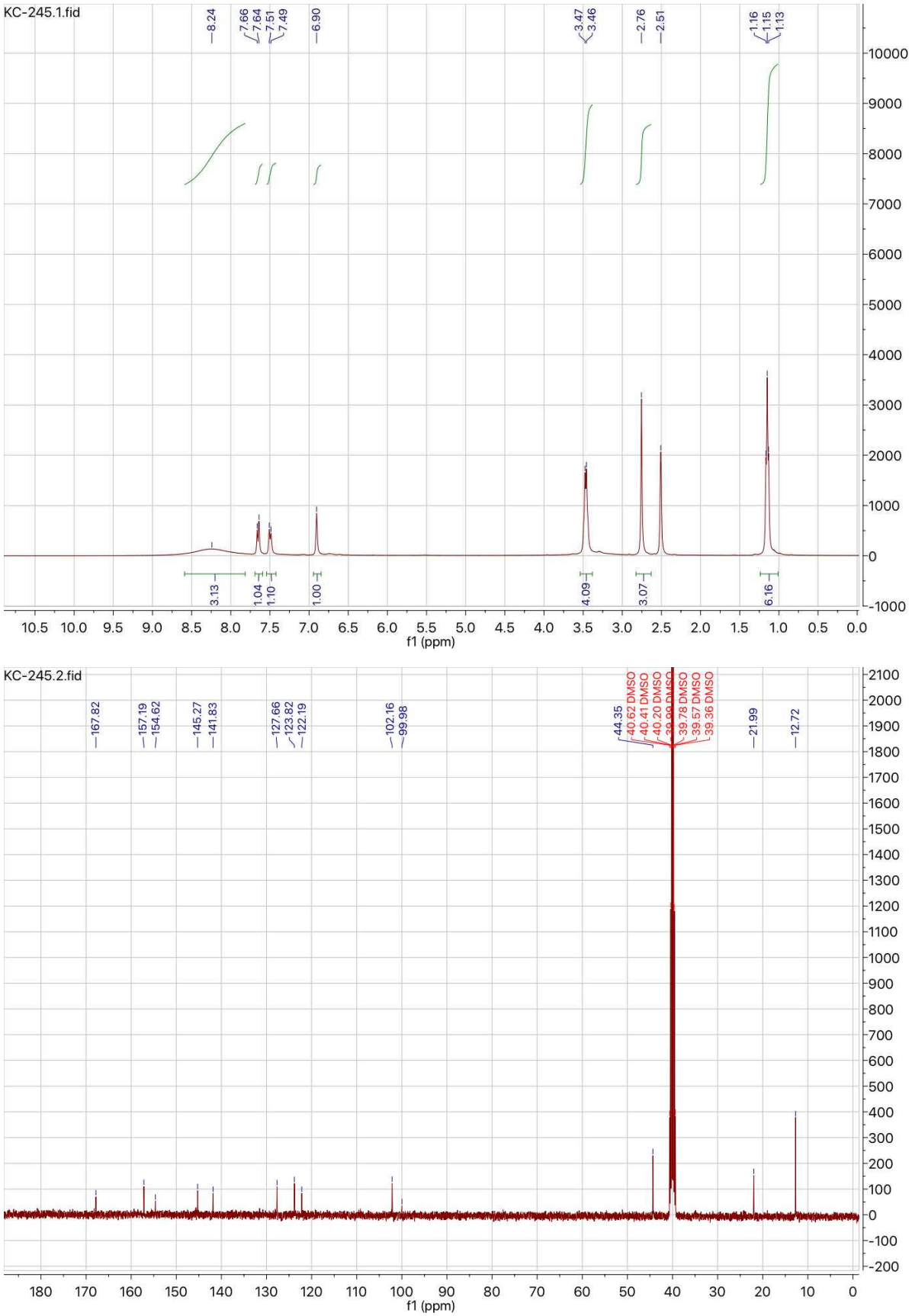

^{1}H and ^{13}C NMR of 1-(6-(diethylamino)-4-methylquinazolin-2-yl)guanidine (**3b**).

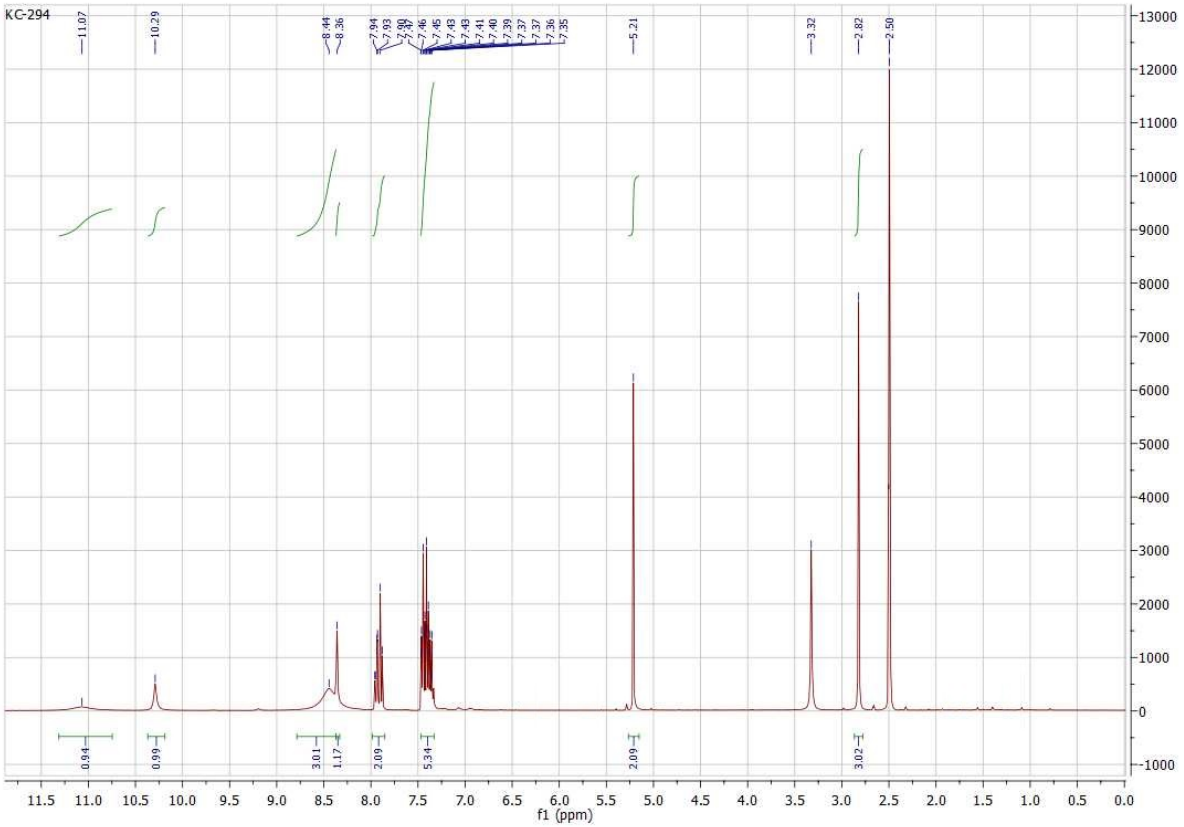

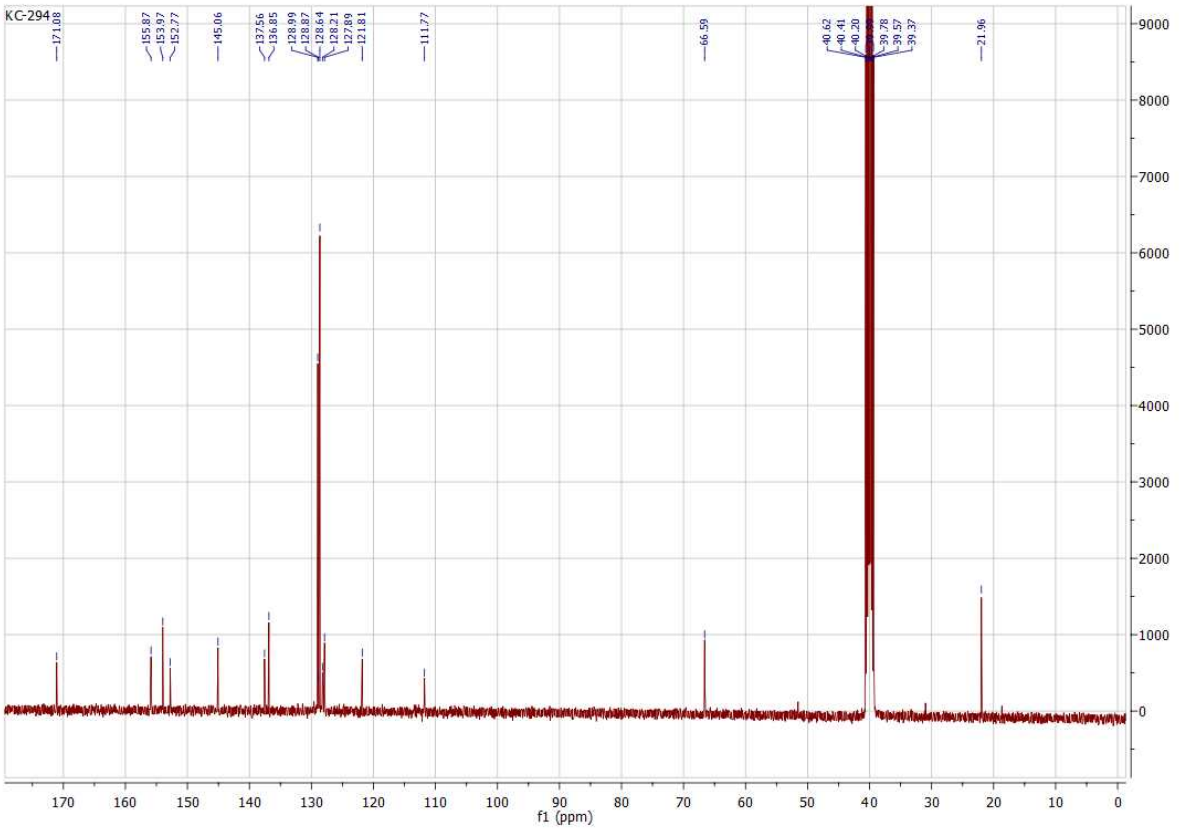

^{1}H and ^{13}C NMR of benzyl (2-guanidino-4-methylquinazolin-6-yl)carbamate (**3c**).

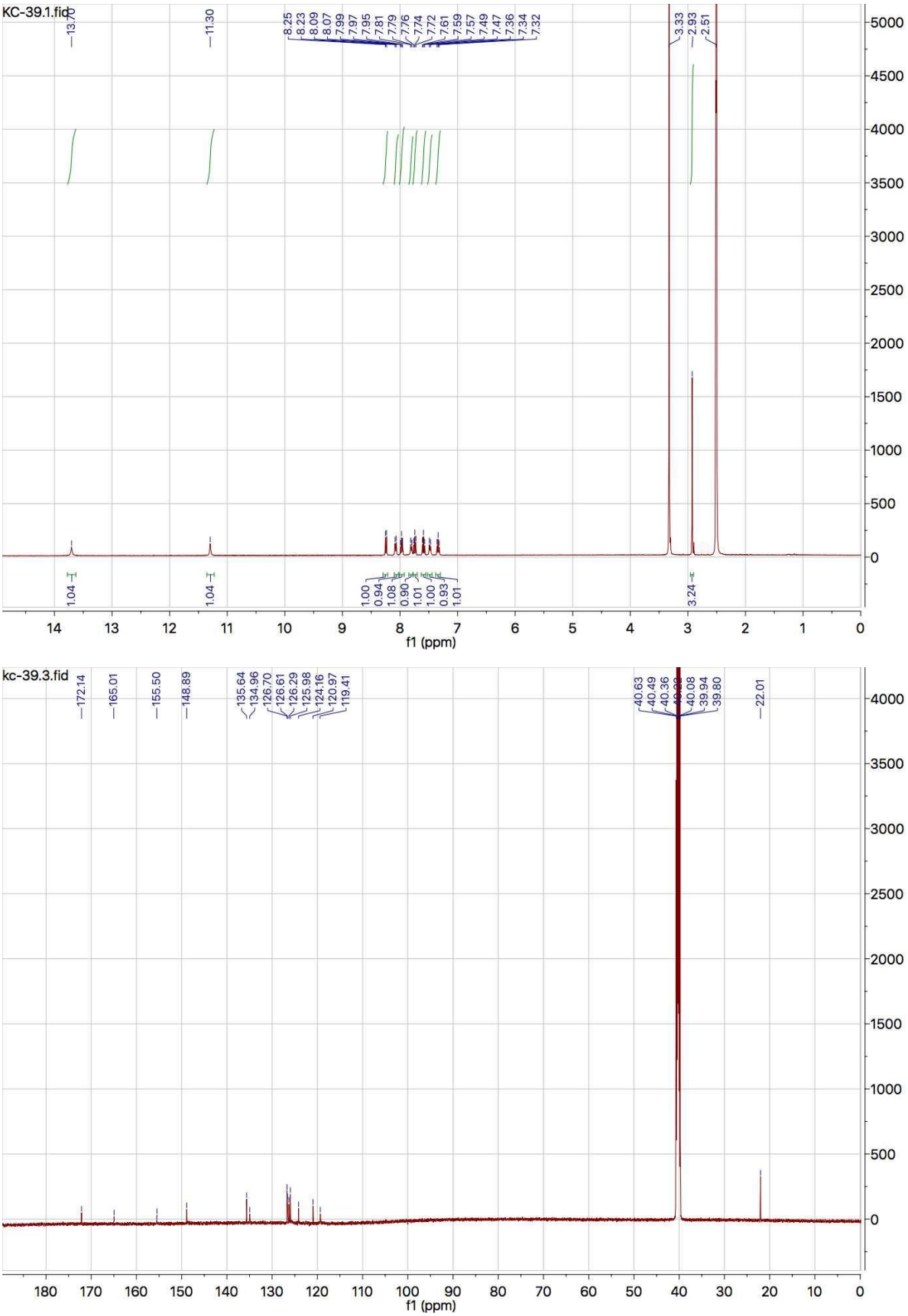

^{1}H and ^{13}C NMR of 2-(4-Methyl-quinazolin-2-ylamino)-quinazolin-4-ol (**4a**).

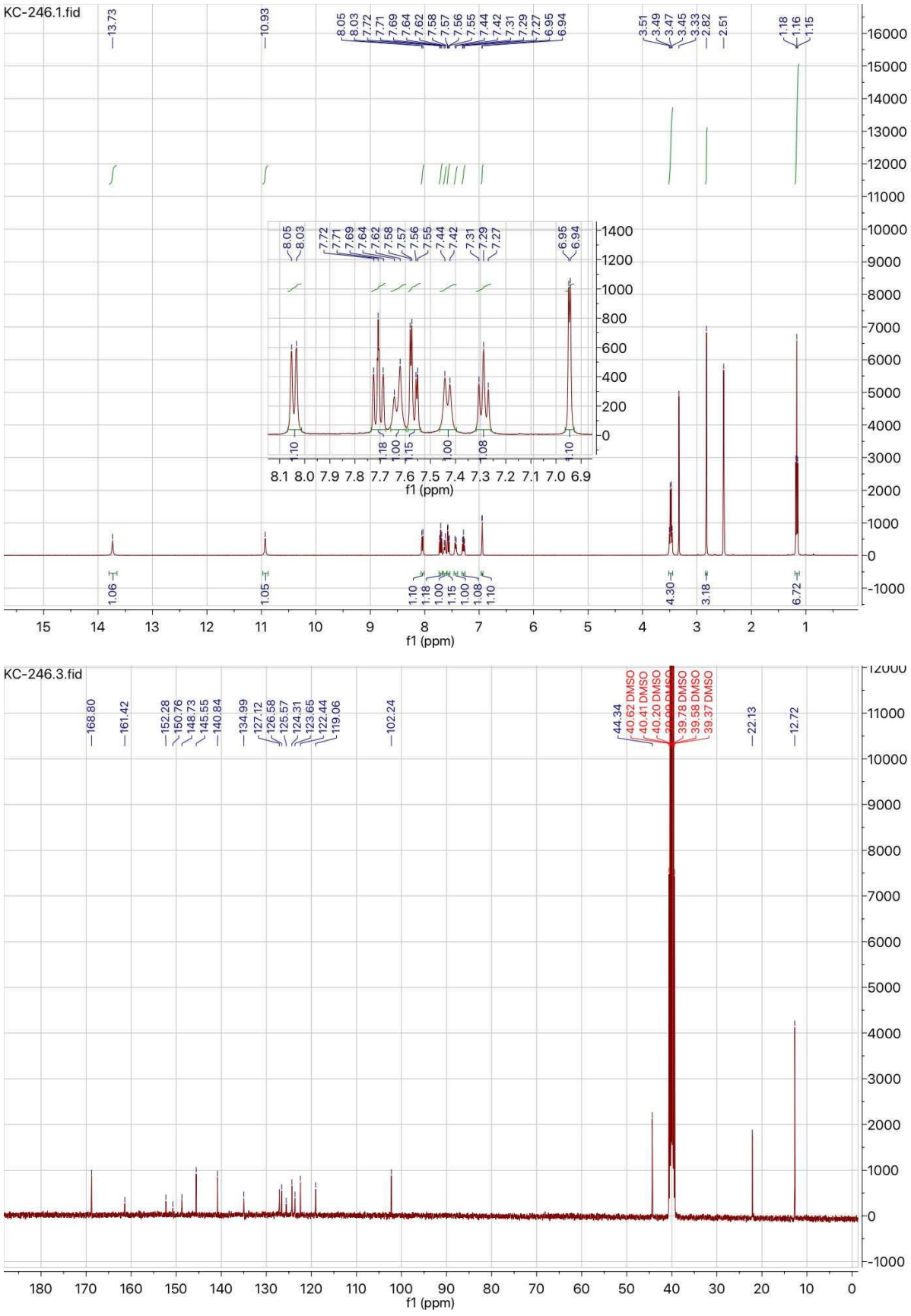

^{1}H and ^{13}C NMR of 2-((6-(diethylamino)-4-methylquinazolin-2-yl)amino)quinazolin-4(1*H*)-one (**4b**).

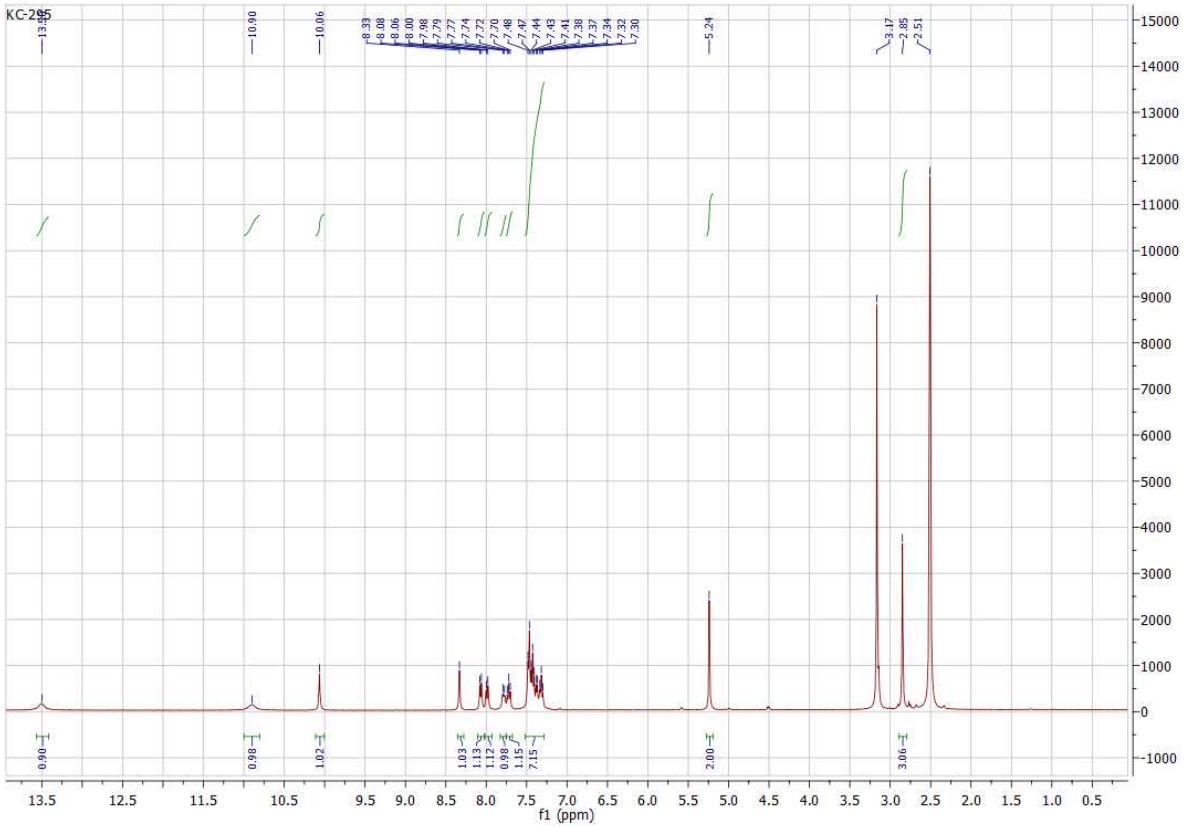

^{1}H NMR of Benzyl(4-methyl-2-((4-oxo-1,4-dihydroquinazolin-2-yl)amino)quinazolin-6-yl)carbamate (**4c**); ^{13}C NMR is not obtained due to poor solubility of this compound.

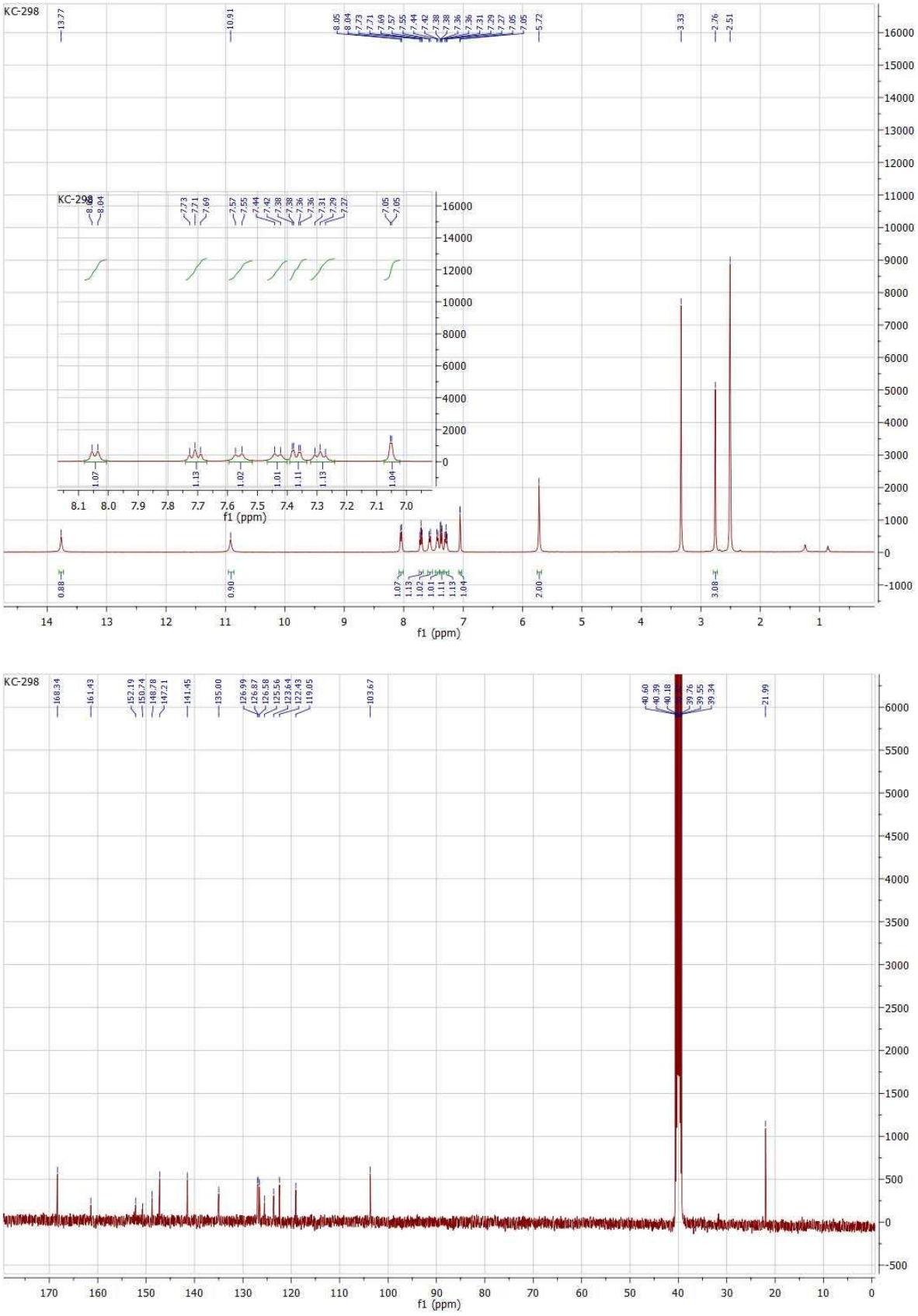

^{1}H and ^{13}C NMR of 2-((6-amino-4-methylquinazolin-2-yl)amino)quinazolin-4(1H)-one (**4d**).

HRMS Spectra of **4a-d:**

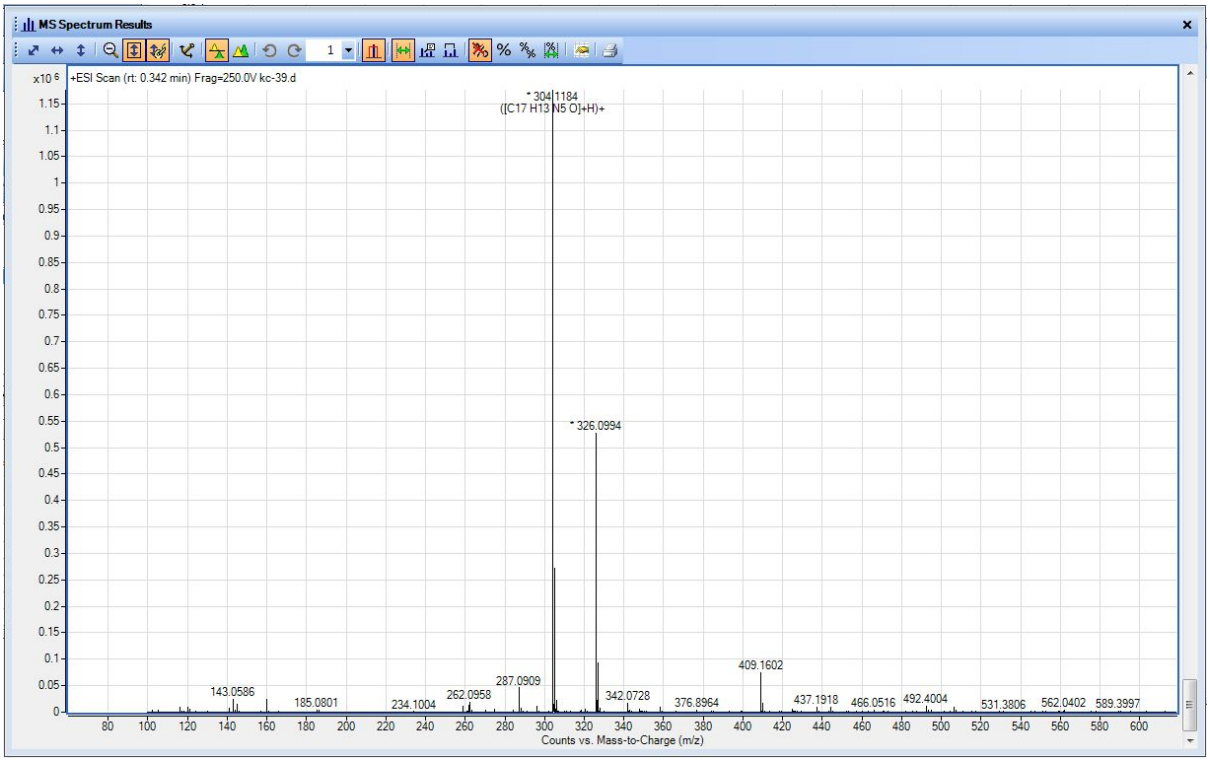

HRMS spectra of **4a**.

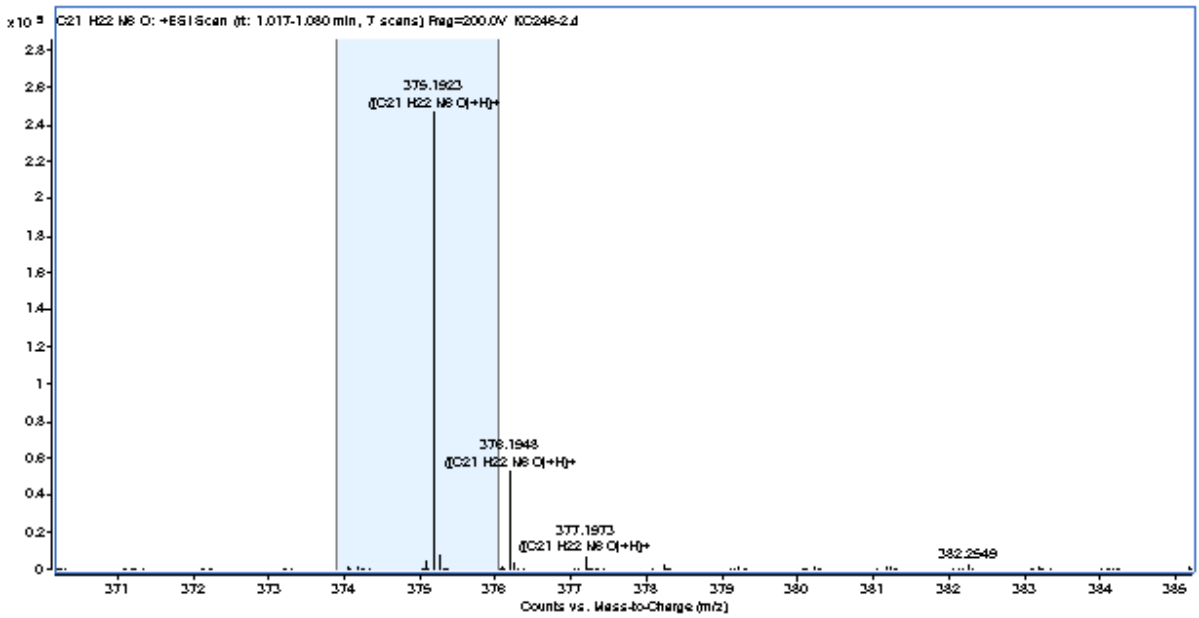

HRMS spectra of **4b**.

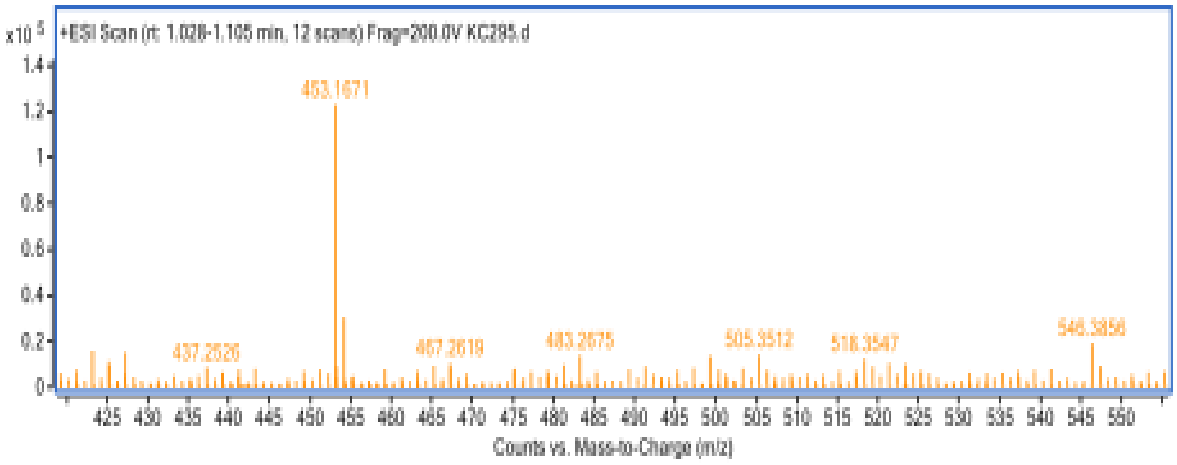

HRMS spectra of **4c**.

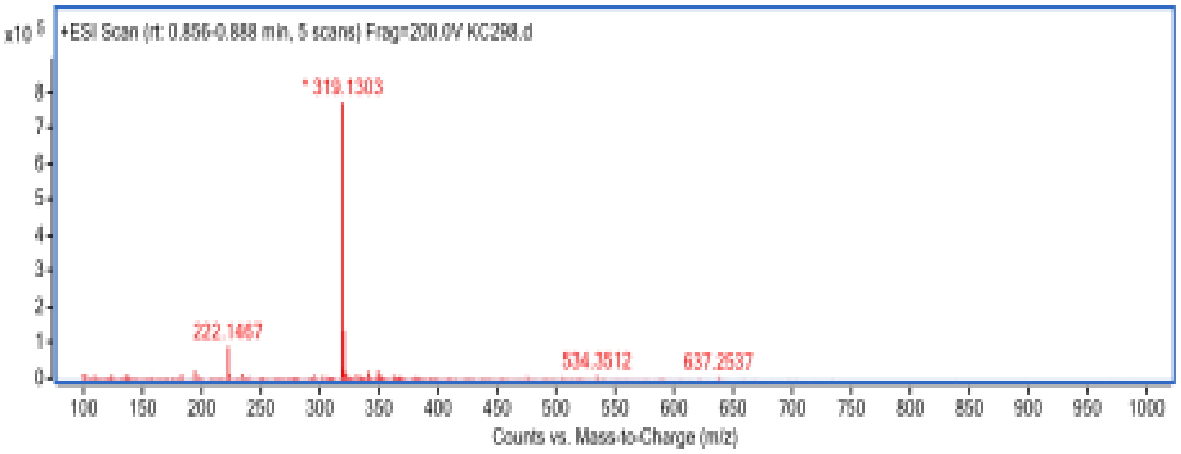

HRMS spectra of **4d**.

References

[S1] P. Thordarson, *Chem. Soc. Rev.* 2011, **40**, 1305–1323.

[S2] L. K. S. von Krbek, C. A. Schalley and P. Thordarson, *Chem. Soc. Rev.* 2017, **46**, 2622–2637.

[S3] V. Grande, C. -A. Shen, M. Deiana, M. Dudek, J. Olesiak-Banska, K. Matczyszyn and F. Würthner, *Chem. Sci.* 2018, **9**, 8375–8381.

[S4] D. D. Le, M. Di Antonio, L. K. M. Chan and S. Balasubramanian, *Chem. Commun.* 2015, **51**, 8048–8050.

[S5] M. Zuffo, A. Guédin, E. -D. Leriche, F. Doria, V. Pirota, V. Gabelica, J. -L. Mergny and M. Freccero, *Nucleic Acid Res.* 2018, **46**, e115.

[S6] J. Jamroskovic, M. Livendahl, J. Eriksson, E. Chorell and N. Sabouri, *Chem. Eur. J.* 2016, **22**, 18932–18943.

[S7] R. del Villar-Guerra, J. O. Trent and J. B. Chaires, *Angew. Chem. Int. Ed.* 2017, **57**, 7171–7175.

[S8] J. -L. Mergny, J. Li, L. Lacroix, S. Amrane and J. B. Chaires, *Nucleic Acid Res.* 2005, **33**, e138.

[S9] V. G. Panse, P. Vogel, W. E. Trommer and R. A. Varadarajan, *J. Biol. Chem.* 2000, **275**, 18698–18703.

[S10] O. I. Afanasyev, A. A. Tsygankov, D. L. Usanov and D. Chusov, *Org. Lett.* 2016, **18**, 5968–5970.